TIME DOMAIN REFLECTOMETRY FOR MEASURING

VISCOELASTIC PROPERTIES

By

O'NEILL JAMES BURCHETT

Bachelor of Science
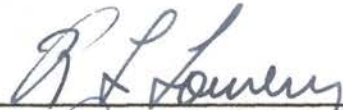Oklahoma State University
Stillwater, Oklahoma
1958

Master of Science
Oklahoma State University
Stillwater, Oklahoma
1960

Submitted to the Faculty of the Graduate School of
the Oklahoma State University
in partial fulfillment of the requirements
for the degree of
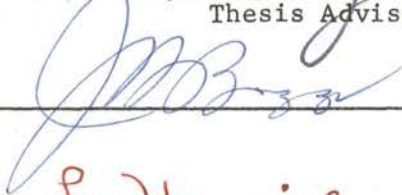DOCTOR OF PHILOSOPHY
May, 1966

TIME DOMAIN REFLECTOMETRY FOR MEASURING

VISCOELASTIC PROPERTIES

Thesis Approved:

_____
Thesis Adviser

_____

_____

_____

_____
Dean of the Graduate School

ii 621472

ACKNOWLEDGMENTS

The author wishes to express his thanks and to acknowledge his indebtedness to the people instrumental in the completion of this study.

Particular appreciation is expressed to the thesis adviser, Dr. R. L. Lowery, for his guidance and patience. The author wishes to thank Dr. J. H. Boggs for his extreme patience and also for making the completion of this study possible. Thanks are due the other committee members, Dr. E. L. Harrisberger and Dr. H. S. Mendenhall.

An expression of thanks is due to the typists Mrs. Lynn Bowles and Mrs. Susan Birmingham and also to the English reader Mrs. Roberta Bose.

I wish to thank my wife and son for the inspiration they have given me during this long study.

TABLE OF CONTENTS

LIST OF TABLES

LIST OF FIGURES

CHAPTER I

INTRODUCTION

The prediction of the behavior of a material under load can be made only if information regarding the elastic properties and strength characteristics is available. Moreover, this information on the strength characteristics and elastic properties must apply to the situation in which the material is to be used. The basis of any prediction of this nature depends upon the assumption that if a material exhibits a certain behavior under load, it will again exhibit the same behavior at a later time if the same loading conditions occur. Since engineering materials do exhibit the same behavior within desired limits under identical loading conditions, the repeatable quantities are called properties of the material. Some common properties of materials are the modulus of elasticity, modulus of rigidity, proportional limit, hardness, yield point, yield strength, tensile strength, Poisson's ratio, toughness, etc. Wide usage of the properties of a material requires a standardization of the test method to determine the properties. This allows a comparative rating among materials.

Properties such as complex moduli, various measures of energy absorbed during impact fracture, and material damping were developed to predict the behavior of a material as additional information was necessary.

1

The most common test method utilizes a loading that is essentially static. Under this type of loading, the measured quantities could be used to predict the behavior of a statically loaded structure. A structure loaded by impact loads or by periodic loads would require extended information to accurately predict the behavior of the structure. The general types of testing developed were static, impact, dynamic (includes forced and free vibrations), creep, fatigue, and ultrasonic.

The behavior of a material such as rubber under a static load is noted to be quite different from steel. During a long time period, rubber flows or creeps much more than steel. The mathematical models such as the Maxwell model were derived to explain the behavior of the rubber. Springs and viscous dash pots are the components of these models. The energy loss (closely resembling viscous fluid flow losses) resulting when the rubber is strained classifies the behavior of the rubber differently from steel's. The term viscoelastic is generally applied to materials whose behavior is similar to rubber's. The internal damping represented by the dash pots in the mathematical models is commonly called the material damping. All materials have some internal damping, but the degree exhibited by each material varies widely.

In any type of testing method, certain assumptions must be made in order to calculate the commonly known properties. For example, the determination of the modulus of elasticity of a material from the standard tensile test is accomplished by measuring the size of the sample. From the measured quantities the modulus of elasticity can be computed assuming the material is isotropic and obeys Hooke's law. (See Appendix A for

the number of quantities that must be measured to determine the properties of a material.)

The available size of the material sample often dictates the method of testing that must be used to determine the physical properties. A few grams of a new elastomer formulated in a laboratory may be impossible to test using a tensile testing machine. Likewise, a polymer dissolved in a solvent may be extremely difficult to test using standard techniques. A very hard material such as a diamond cannot be shaped into a standard size test specimen to determine its properties.

There have been a number of materials testing techniques, including ultrasonic testing, developed to measure various materials. Nolle [26]* discusses several methods for measuring the dynamic properties of visco-elastic (rubber-like) materials. These methods include: the rocking-beam oscillator, which has a nominal test frequency range of 0.1 to 25 cps; the vibrating reed method, which covers the test frequency range of 10 to 500 cps; the strip transmission method, which can be used in the frequency range of 1 to 40 kc; the strip resonance method, whose frequency range is wholly determined by the properties of the material; and the magnetostriction method, which can be used in the frequency range of 12 to 120 kc. In addition to those named by Nolle, the low frequency test methods also include the forced and free vibration technique. All of these test methods were developed to examine the behavior of a material.

A viscoelastic material possesses moduli which have real and imagi-nary components. The standard tensile tester does not measure a suffi-cient number of independent quantities to determine the complex moduli.

---

*Numbers in brackets refer to references in the Selected Bibliography.

The test methods mentioned by Nolle were developed to measure properties such as the complex moduli. These test methods also allow a study of the variation of physical properties when the test frequency and/or ambient temperature are changed.

Rubber is one of the common viscoelastic materials. Before synthetic rubbers and polymer plastics were developed, the rubbers were the principal viscoelastic materials, and all testing procedures were developed to evaluate the viscoelastic properties of the rubbers. These tests were the creep tests under constant load and the stress-relaxation tests (constant strain). The period of time required to perform these tests led to the development of many relationships such as the connections between time and temperature. These tests and other relationships are explained by Bergen [1] and Ferry [3].

All materials have viscoelastic properties, but the degree to which they behave in a viscoelastic manner, of course, varies from material to material. The tests developed to determine viscoelastic properties of rubbers are not directly applicable to such materials as steels. The development of viscoelastic models (Maxwell, Voight, etc.) allows the determination of viscoelastic properties regardless of the type of test involved since the idea is to determine the values of the components of a model.

The theories of elasticity and acoustics are the basis for the determination of physical properties from wave propagation characteristics. The basic relationships between physical properties and wave propagation characteristics can be found in the works of Kolsky [4], Love [7], and Mason [9]. Therefore, the determination of physical properties using

ultrasonics is accomplished by measuring wave propagation character-
istics.

The term ultrasonic generally refers to an acoustic wave which has
a frequency above the hearing range of man. That is, the possible range
of the ultrasonic frequencies is from 20,000 cps to an upper limit deter-
mined by the domination of an electromagnetic wave rather than by an
acoustic wave. The basic ultrasonic testing method involves the genera-
tion of an ultrasonic acoustic wave which propagates through a material.
From this generated wave the velocity of propagation is determined along
with the attenuation of the wave amplitude.

There are four basic wave modes possible--longitudinal, shear, sur-
face, and Lamb. The two basic particle motions relative to the direction
of wave propagation are transverse and longitudinal (in the same direc-
tion as propagation). These motions define the shear and longitudinal
wave modes respectively. Other wave modes consist of particle motions
which are combinations of the shear and longitudinal modes. The shear
wave and the longitudinal wave are used to determine physical properties.
With these two waves four distinct quantities can be measured--two veloc-
ities of propagation and two wave attenuations. In addition, the frequency
of the wave is also known as are the test sample dimensions (physical
size). The density of the test material is also considered known. With
these quantities the complex moduli can be calculated for an isotropic
material which obeys Hooke's law.

Since the ultrasonic testing method basically consists of measuring
wave frequency, velocity of propagation, and attenuation, all innovations
on an ultrasonic test method must still use these basic test measurements

or related quantities. The simplest ultrasonic tester consists of an acoustic wave generator (transmitter) and an ultrasonic wave receiver. These are placed on opposite sides of a material and the time necessary for the wave to traverse the material is measured. The decrease in amplitude of the wave entering the material and the wave amplitude as it reaches the opposite side determines the wave attenuation. This type of testing is called the through-transmission method.

A variation of the through-transmission method is called the interferometer method in which a second ultrasonic path is used. Two transmitters and two receivers are used. The simplest form of this method uses one wave path to determine the references for time and wave attenuation by placing one receiver directly in contact with one of the senders. Both transmitters (senders) must be pulsed simultaneously. The second acoustic path is often a water bath or water-alcohol bath because the speeds of sound in water and alcohol are accurately known and they vary little with temperature. The length of the acoustic path in the water bath is adjusted until the time of the wave travel is the same as that in the test sample path which determines the time for the wave to traverse the test sample. The basic through-transmission ultrasonic system is explained in the work of McGonnagle [8].

Most of the test systems developed use buffer blocks. The buffer blocks inserted between the crystals and the sample do not affect the theory of operation, but they are inserted for two reasons; to furnish a physical separation between the crystal isolating the sample ambient temperatures from the crystal or isolating the sample detachment stresses from the crystal and to separate in time the arrival of shear and

longitudinal waves simultaneously generated by the sending crystal. The
separation in time at the end of the buffer block occurs because the two
wave modes travel at different characteristic velocities.

The basic pulse-echo testing method described by McGonnagle [8] uses
a single transducer which is both transmitter and receiver for the ultra-
sonic waves. The operation consists of pulsing the transmitter to produce
the acoustic wave which travels through the test material (buffer block
also if included), strikes the opposite side of the test material, and is
reflected back to the transmitter which is used as the receiver. The
length of wave path and the time of travel are measurable and determine
the velocity. Attenuation of the wave amplitude is determined by meas-
uring the amplitudes of successive echos of the initial wave. Inter-
ferometer or two path systems can be used but do not reap the advantages
gained in through-transmission systems.

Another test method, explained by Schneider and Burton [33], uses a
rotating plate to determine the angles of complete reflection of an
impinging ultrasonic wave. The theory of operation of this method is
also explained by McGonnagle [8].

The further development of the art of ultrasonic testing consists of
innovations of the methods mentioned--all of which increase the accuracy
or ease of operation. Many of the specialized methods gain a higher
degree of accuracy but greatly complicate the procedure of testing.

The advantages and disadvantages of each test method render some more
applicable to certain materials than others. Of the basic methods, the
pulse-echo method has the following advantages:

1. It has simplicity of operation with minimum components.

2. The multiple reflections from within the test sample make attenuation measurements simple.

3. Only one sample interface is necessary when the sample is coupled to the transducer.

4. It can be used with direct sample coupling or with immersion testing.

5. No problems of mismatch between transmitting and receiving crystals are encountered.

The disadvantages of the pulse-echo system are:

1. The wave must traverse the sample thickness twice with a reflection at the sample-air interface. This requires that a highly damped (lossy) material must be extremely thin. The thinner the sample the more chance there is for thickness measurement error.

2. The reflection at the sample-air interface causes a phase shift of the wave which may complicate time measurements.

3. If the side of the sample opposite to the transducer has a water backing, then a portion of the wave energy is transmitted through. This makes attenuation measurements difficult.

4. Testing with shear waves using a buffer block is extremely difficult because the reflected longitudinal mode almost coincides with the shear mode in time of arrival at the receiver.

5. The receiving amplifiers must withstand the pulse voltage applied to the crystal and then amplify the small voltage echo received.

The through-transmission system has the following main advantages:

1. No reflecting surface for the wave is necessary.

2. A thicker sample can be used than is possible with the pulse-echo system. This makes length measurements more accurate.

3. No problems are encountered with longitudinal wave reflections in the buffer block when shear waves are used.

4. Extremely small orders of error in velocity measurements are possible with simple interferometer techniques.

5. Receiver crystals are separate from transmitters so that amplifiers in the receiving line are not subjected to high pulse voltages.

The through-transmission system has the following disadvantages:

1. More equipment is necessary including an extra receiving crystal.

2. A time reference for velocities must be established since a reflection from the buffer block-sample interface cannot be used.

3. Sender and receiver crystals must be matched or calibrated.

The rotating plate method, which is a through-transmission method, uses a liquid couplant between the transmitter and the sample disc (immersion technique). The liquid couplant will not support a shear wave although a longitudinal wave striking the plate at an angle will convert into two modes to produce a shear wave in the sample. The shear wave must traverse the sample and then enter the liquid couplant between the sample and the receiver. Since the liquid will not support a shear wave, a longitudinal mode conversion must occur in order to receive any signal from a shear wave in the sample.

The possible error in location of the immersed transmitter and receiver makes the method unsuitable for extreme accuracy in the determination of velocities. Also, the determination of wave attenuation values can be

accomplished only if the reflected portions of the wave are known along with the attenuation produced by the couplant fluid.

The two-path through-transmission method of ultrasonic testing was selected for testing highly attenuated (lossy) materials because the transmitting crystals could be driven at extremely high voltages without damage to sensitive amplifiers in the receiving circuit. Also, the system could use shear wave transmitters without the inherent complication of reflected longitudinal waves in the buffer blocks covering desired signals. In addition, the highest possible accuracy could be obtained simply through use of high quality instrumentation. A suitable general schematic of the test system is shown in Figure 1.

The test schematic of Figure 1 is an interferometer method using two acoustic paths. The system consists of an ultrasonic pulser which simultaneously drives two matched quartz crystals (transmit or send units). The frequency of the gated sine wave corresponds either to the fundamental natural frequency of the crystals or to an odd harmonic of their fundamental frequency. The two matched sending crystals generate an acoustic wave in each path which travels to the buffer block-sample interface where a portion of each initial wave propagates through each of the two samples. The wave in each path is detected by one of two receiving crystals. The two receiving crystals are matched to the two sending crystals. The detected signals are then amplified by identical amplifiers.

The test samples S_1 and S_2 are of identical material and cross-sectional area but differ in thickness by the amount d. Thus, if the acoustic wave reaches receiving crystal 2 before receiving crystal 1,
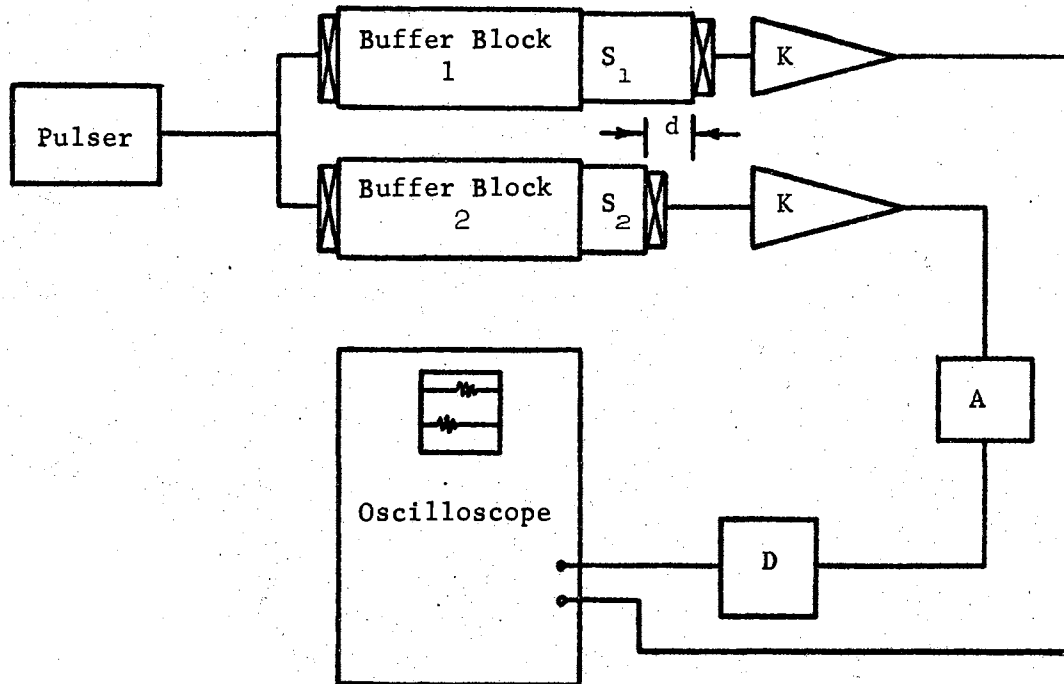
Figure 1. Improved Ultrasonic Interferometer Test Schematic.

the signal received at crystal 2 will be of larger amplitude since it has traveled a shorter distance through the sample.

A variable attenuator (A) and a variable time delay unit (D) are placed in path 2. The signals from each receiver are displayed on a dual-trace oscilloscope so that the amplitudes of the two traces can be equalized. The calibrated attenuator reading gives the attenuation due to the thickness d when the two signals are adjusted to the same amplitude. The calibrated variable delay unit is adjusted until the two traces are at the same horizontal (time) position to determine the time of travel of the wave in a thickness d of the test material. The velocity of the wave and the attenuation per unit length can now be determined for the test material.

The interferometer technique of Figure 1 differs from most systems in that it has test material in path 2 rather than using water or the absence of material between the sender and receiver. The addition of a thinner test sample in path 2 assures the same number of interfaces in each acoustic path, thus eliminating phase shift and couplant attenuation problems.

The methods of testing discussed up to this point were investigated as background for the development of a method of testing lossy materials ultrasonically. Experimental tests using the basic methods established that further innovations in these methods were not the solution to the problem of developing a test method for lossy materials. Therefore, the general method outlined in Figure 1 was chosen as the basic testing method most suitable for testing the lossy material which had been selected as a norm. Cunningham and Ivey [7] have already established the accuracy limits of the test method of Figure 1. The real problem which arose in the testing of extremely lossy materials was to obtain readable data. Therefore, the limits of the testing method were selected by choosing a lossy material (urethane) in which previous tests failed to obtain data. Conditions for testing the urethane were selected which were well outside the bounds previously established. The cause of failure in previous tests was determined to be the failure to produce an acoustic wave of sufficient amplitude to traverse the test sample.

The problem is to extend the test method so that both longitudinal and shear waves will traverse the test material and readable data can be obtained. It has already been established that the basic test method is sufficiently accurate and simple to operate. There is a basic need for

a method capable of testing materials heretofore untested under stipulated conditions to increase the knowledge of the behavior of the material. To accomplish this end, the specific problem to be solved in this study is to develop a through-transmission ultrasonic test system capable of traversing a selected urethane material. The solution of this problem requires the following:

1. A more intense shear wave must be generated in order to penetrate the urethane samples which had a thickness of approximately 0.156 inches.

2. The problem of multiple reflections within the buffer block and mode conversion signals and their reflections must be analyzed and interpreted to insure ability to locate a specific wave signal.

3. The problem of mode conversion at the buffer block-test sample interface must be analyzed and then minimized.

CHAPTER II

STATEMENT OF THE PROBLEM

This study involves the development of a method of testing highly

damped viscous materials such as urethane. A highly damped material is

herein described as a material which highly attenuates an ultrasonic wave--

100 db per inch minimum.

The general scope of this work is to develop a test method which

would be capable of testing lossy (highly attenuated) materials under con-

ditions which have until now prevented their testing by ultrasonic means.

Ultrasonic testing of lossy materials is generally limited to the

determination of the complex modulus of elasticity and the complex shear

modulus of elasticity. This requires that data be obtained on the veloc-

ity of wave propagation, the attenuation of the wave, and the frequency

of the wave for both longitudinal and shear waves. A shear wave differ-

entiates from a longitudinal wave in that particle motion is transverse

to the direction of wave propagation.

The viscous properties of a lossy material become more dominant as

temperature increases. A lossy material gradually loses its viscous prop-

erties as temperature decreases. This lowers the degree of ultrasonic

wave attenuation as the temperature is lowered and vice versa. Therefore,

a lossy material may be tested at low temperatures with a given ultrasonic

wave intensity whereas testing at higher temperatures with the same wave

intensity may be impossible due to increased damping. An example of this appears in Chapter V where Van Valkenburg states that some urethanes were not tested ultrasonically above -10°C and above frequencies of 1 megacycle per second because the ultrasonic wave was completely damped as it traversed the urethane. The damping of a lossy material increases as the frequency of the ultrasonic wave increases. The relation between an increase of frequency and damping is found in Equations (12), Appendix A.

A lossy material such as urethane could be used in a structure subjected to temperatures below and above standard ambient conditions. The behavior of the material as the temperature is varied needs to be determined to facilitate design procedures. The lossy materials certainly could be used in structures subjected to temperatures in the neighborhood of 20°C.

A method of testing lossy materials such as urethanes needs to be developed to determine their properties under the conditions of temperatures above -10°C and frequencies of 1 megacycle per second. The behavior of a viscoelastic material changes as the frequency changes. Thus, an increased ultrasonic test frequency range would add to the information known about a material. Most viscoelastic materials possess properties which have a maxima relative to variation in frequency or temperature.

The success of the attempts to test the urethane samples was found to depend upon two factors: generating a high intensity shear wave in the test sample, and developing and using reflection diagrams for the ultrasonic waves detected by the receiving crystal. The first factor basically consisted of the development of electronic components capable

of driving a high impedance crystal at a high power level. A 2000 volt pulse (peak-to-peak) was found to be a minimum in preliminary tests. No system is available commercially in this voltage range. The impedance matching methods used in radio transmitters were adapted so that the transmitting crystals could be remotely located from the power oscillator. The generation of the shear wave in a test sample also required control of buffer block material, wave scatter phenomena, and face parallelity. The second factor (reflection diagram interpretation) concerned a method of locating the approximate oscilloscope time position relative to the initial pulse of a shear wave traversing the test sample. The shear wave was very highly damped in comparison with longitudinal waves. Therefore, the received shear wave usually was of no larger amplitude than longitudinal waves reflected several times. The problem is to identify which signal is the shear wave. No reference to this method was found in literature. This would then classify the test method developed here as unique although the block diagram would not present any new components. It should be noted that the electronic components constructed developed driving voltages at the crystal much higher than any given in literature or commercially available.

The development of a gated sine wave with a fast rise and fall time requires special efforts. A tuned circuit, which is necessary to drive the crystals, rings for $Q/3$ cycles. With Q-values (ratio of maximum power stored per cycle to maximum power dissipated) of 100 this would be 33.3 cycles. At 2.25 megacycles it would then require 15 microseconds for the oscillation amplitude to decay to 36% of its initial amplitude. A usable pulse length for testing is less than 5 microseconds since a

long pulse length would allow longitudinal waves to cover shear waves. Obviously a method of damping the circuit must be used.

CHAPTER III

ULTRASONIC WAVE MODE CONVERSION AND REFLECTION

IN CONNECTED MEDIA

A metal buffer block possesses shear and longitudinal wave velocities which differ by a factor of approximately two. If a metal test specimen is also used, many complicated reflections appear. A reflection diagram is shown in Figure 3 for the system pictured in Figure 2.
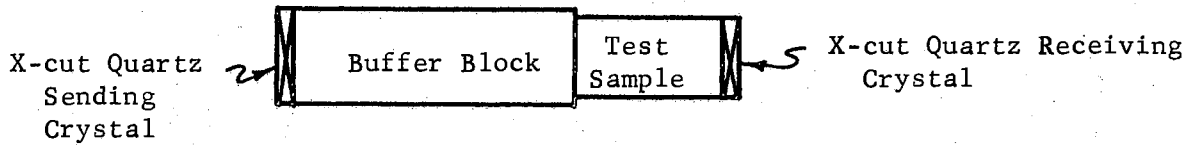
Figure 2. Longitudinal Wave Through (Transmit--Receive) System.
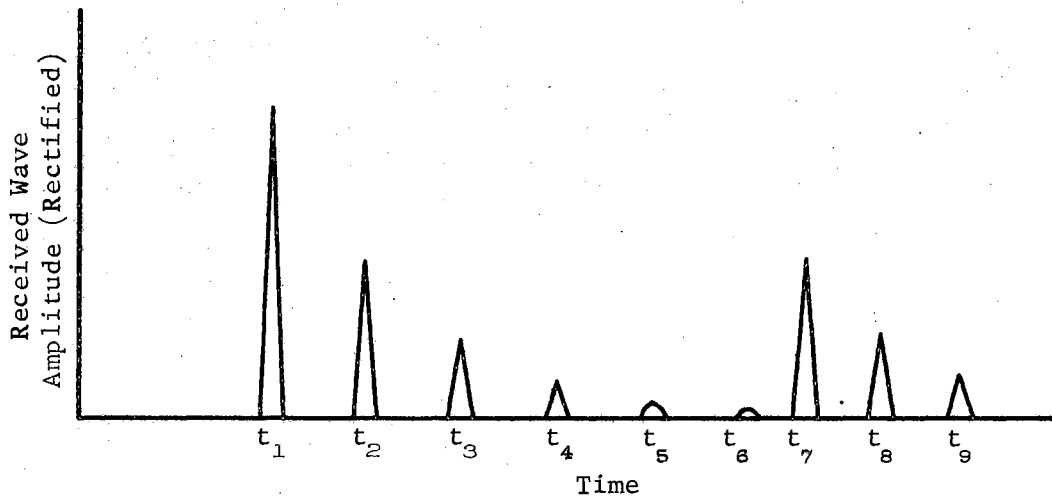
Figure 3. Reflection Diagram for System of Figure 2.

for t_1

for t_2

for t_6

for t_7

for t_9
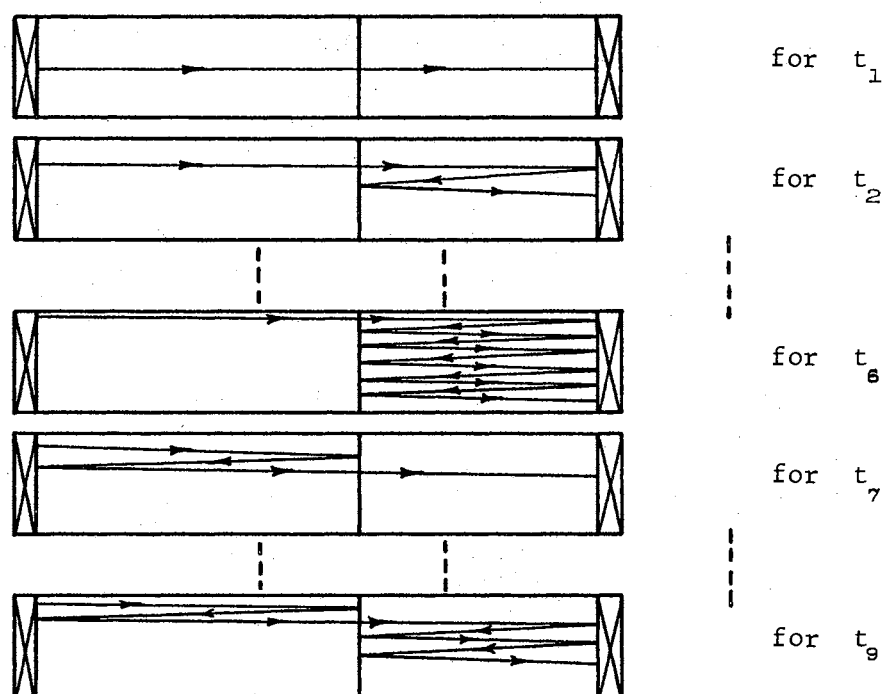
Figure 4. Wave Paths for Reflection Diagram of Figure 3.

The reflections which appear at times t_1, t_2, t_3, . . ., t_9 are pictorially represented in order in Figure 4.

When the sending and receiving crystals of Figure 2 are replaced by Y-cut crystals, a reflection diagram similar to Figure 5 could appear.

The signal detected at time t_1 (Figure 5) is the longitudinal wave. The signal at time t_3 (Figure 5) is the longitudinal wave reflected in the buffer block. All other noncross-hatched signals are reflections within the sample. The wave at t_2 (Figure 5) is the shear wave. The remaining cross-hatched signal is a shear wave reflected within the test sample. The wave paths for each signal can easily be determined by using the system in Figure 4.

The buffer block should allow an acoustic wave to travel into the test sample with no mode conversion at the interface as long as the
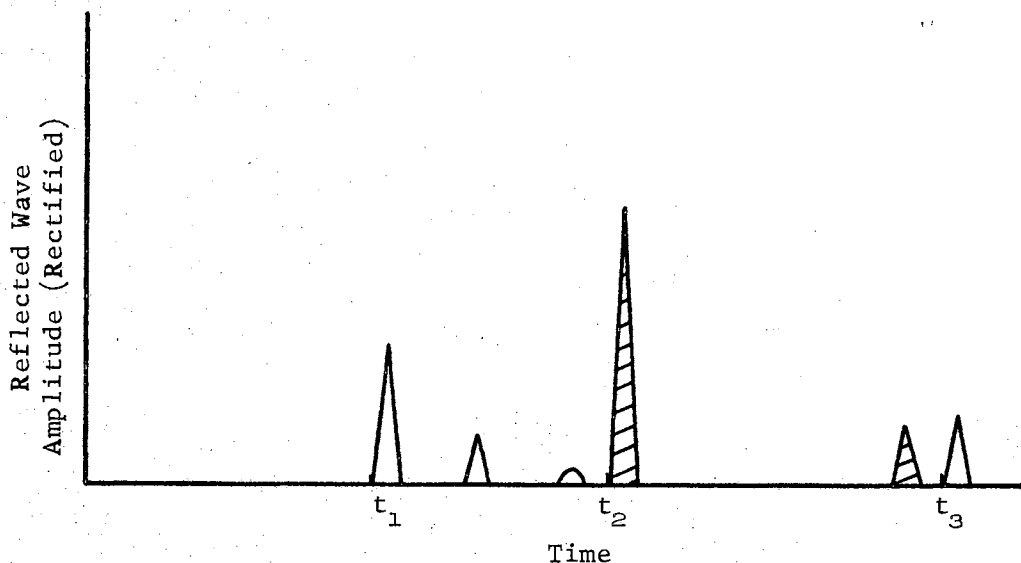
Figure 5. Shear Wave Signals.

opposite faces of the buffer block are parallel and flat according to
Snell's law. If the faces are not parallel, then mode conversion occurs
as is shown in Figure 6. The existence of the shear wave and longitudinal
wave modes at an interface is proven by the application of existing bound-
ary conditions to the wave equations. Snell's law predicts the existence
of two wave modes (longitudinal and shear waves) since their velocities
differ.

The degree of not being parallel is exaggerated in the figure to
better explain the phenomenon. The results of such conditions would be
that both a shear and longitudinal wave would be generated to travel
through the test sample although only a shear wave impinged upon the
buffer block-sample interface. The effects of this situation on the
reflection diagram appear in Figure 7. The additional received signals
result from mode conversion at the buffer block-sample interface.

Buffer Block

Longitudinal Wave

Shear Wave

Test Sample

Shear Wave

Reflected Longitudinal Wave

Reflected Shear Wave
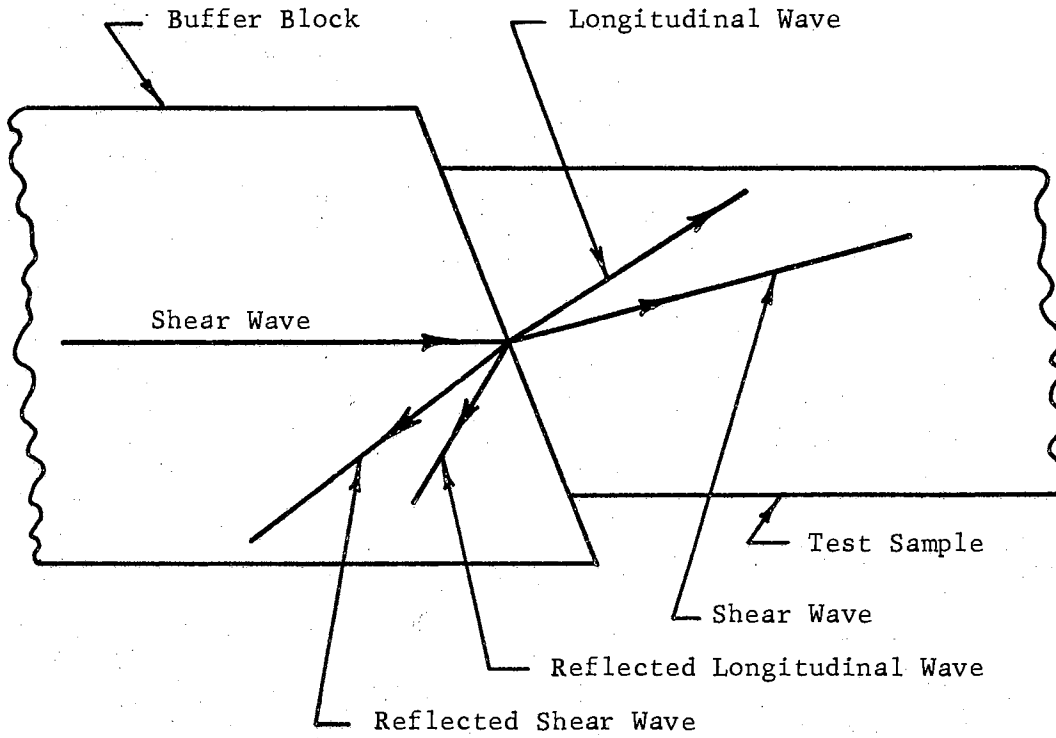
Figure 6. Mode Conversion at Buffer Block-Sample Interface.

Longitudinal Wave From Mode
Conversion

Received Signal
Amplitude (Rectified)

t_1

t_2

t_3

Time
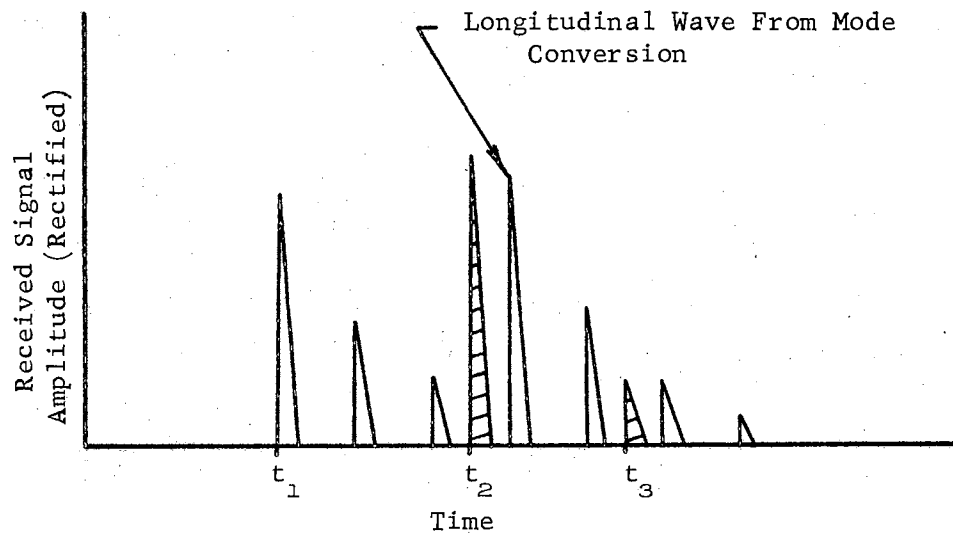
Figure 7. Mode Conversion Reflection Diagram.

The mode conversion at the buffer block-sample interface divides the wave energy which further decreases the intensity of the shear wave. Also, since the longitudinal component is not as heavily damped, it may be received with a greater amplitude than the shear wave. The large number of received signals in addition to the small amplitude of the shear wave makes the location of the shear wave difficult. This condition also increases the difficulty of making material wave attenuation measurements.

An ultrasonic wave generated by a quartz crystal and propagated into a buffer block does not travel in a beam but diverges after it leaves the near field zone. This divergent condition would complicate the measurement of attenuation because of apparent loss of wave energy. In addition, this situation means that the wave front is not plane as it strikes the end of the buffer block. This condition then reduces to the same condition as if the faces of the buffer block were not parallel. Figure 8 roughly presents the situation.
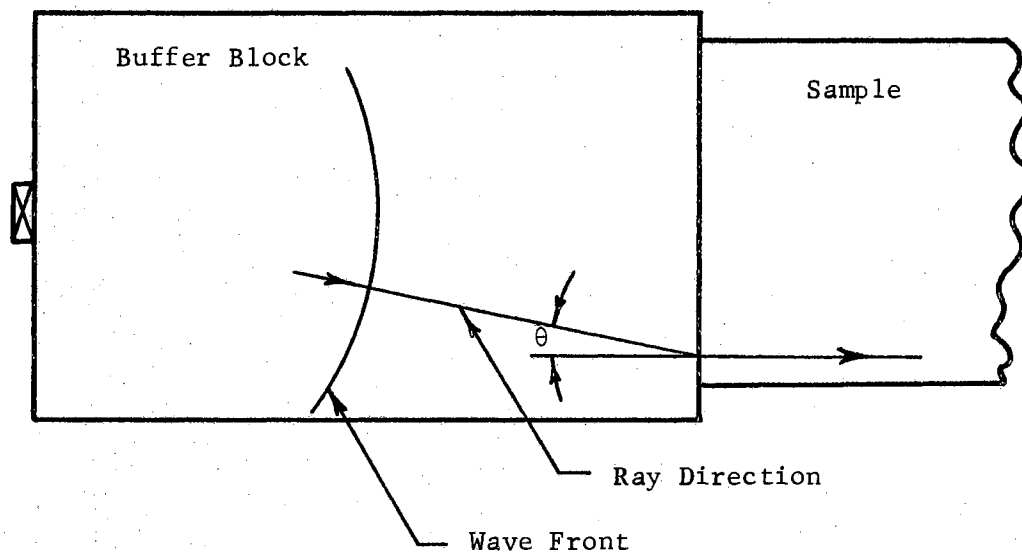
Figure 8. Beam Effects in Buffer Block.

The larger the size of the sending crystal, the less the beam will diverge; also, the higher the frequency, the less the beam will spread. These two factors need to be considered in buffer block design along with the arrival time separation between shear and longitudinal waves impinging on the end of the buffer block. Another possibility would be to use a buffer block that has the same size as the sending and receiving crystals. This would tend to limit any divergence of the beam and deliver all of the wave energy (except that reflected) to the sample. A problem arises here also from a mode conversion phenomena. A Rayleigh or surface wave results from mode conversion and must be dissipated to prevent further confusion in the reflection diagrams.

Another fact to consider in a buffer block design is the degree of isotropy pertaining to wave propagation. Probably the most isotropic material used is fused quartz. In this material scattering at grain boundaries is at a minimum. If materials such as fused quartz or fused silica are not available, a fine grained, low-damping material should be used such as aluminum. It should be noted that in some cases a coarser grained material is preferred. The reason for this is that any divergent rays are supposedly scattered to insignificance.

As an acoustic wave propagates through a material and reaches an interface between the material and a second material, there is a reflection from the interface. The amount of energy reflected depends upon the acoustic impedances of the two materials. The acoustic impedance is defined by $Z = \rho v$ where the system is in absolute units, but ρ is the density of the material and v is the velocity of the acoustic wave. If no standing waves are present, the relationship between intensity of a

wave incident and the intensity of the transmitted wave at an interface is given by

$$I_2 = I_1 \left[\frac{4Z_2/Z_1}{(Z_2/Z_1 + 1)^2} \right].$$

I_2 is the intensity of the wave transmitted into the second medium and I_1 is the intensity of the wave in medium 1 which strikes the interface. Z_1 and Z_2 are the acoustic impedances of materials 1 and 2 respectively. The expression for the intensity of the reflected portion of the wave is:

$$\frac{I_1}{I_{refl}} = \frac{(Z_2/Z_1 + 1)^2}{(Z_2/Z_1 - 1)^2}.$$

The data in Table I give the wave intensities at an interface for several buffer block materials.

The acoustic impedance of most lossy materials such as rubber and urethane is lower than that of Lucite; therefore, the portion of the wave transmitted into the test sample is smaller than any of the portions shown in Table I. (The intensities were calculated from data furnished by McGonnagle [8].)

Another example of impedance mismatch is an aluminum buffer block and a polyethylene test sample. For longitudinal waves 34% of the energy will be transmitted and 66% will be reflected. For shear waves 21% of the energy will be transmitted and 79% of the energy will be reflected. The shear wave is very rapidly damped in the polyethylene; therefore, when the shear wave is only 21% transmitted and then heavily damped, the amplitude of the wave is very small.

TABLE I

TRANSMITTED AND REFLECTED WAVE INTENSITY AT AN INTERFACE

LONGITUDINAL WAVE			
Material 1 (Buffer block)	Material 2 (Test Mat'l)	I_2	$I_{refl.}$
Aluminum (17ST)	Lucite	$.52I_1$	$.48I_1$
Naval Brass	Lucite	$.30I_1$	$.70I_1$
Glass	Lucite	$.59I_1$	$.41I_1$
Quartz (Fused)	Lucite	$.63I_1$	$.37I_1$
SHEAR WAVE			
Aluminum (17ST)	Lucite	$.41I_1$	$.54I_1$
Naval Brass	Lucite	$.27I_1$	$.73I_1$
Glass	Lucite	$.41I_1$	$.54I_1$
Quartz (Fused)	Lucite	$.48I_1$	$.52I_1$

Another case of unwanted reflected waves comes from reflections from the sides of the buffer block. There are two methods of accomplishing a reduction in the effects of the reflected energy. One method would be to place the sides of the buffer block so distant that any diverted wave energy would travel so far that it would not affect measurements since it would take so long to return. The other method would be to scatter the wave to insignificance. This condition of wave scattering can be approached by using a rectangular cross-section block with the crystal mounted slightly off center or by the machining of serrations on the sides of the block to scatter the reflections.

An oscillogram of a 2.25 megacycle ultrasonic wave at the end of a naval brass buffer block is shown in Figure 9. The first signal (moving from left to right) is a longitudinal wave. The second signal is a shear wave. The third signal is a reflection within the buffer block. This reflection is generated by the longitudinal wave as it impinges on the face of the buffer block. The three signals result from pulsing a Y-cut quartz crystal whose fundamental natural frequency is 2.25 megacycles per second. The amplitude of each signal is considerably greater than any extraneous reflection or noise signals. This would facilitate the location of a shear wave of small amplitude.

All of the related values of wave intensity found in this chapter (transmitted or reflected) are theoretical. In actual practice the couplant between the two materials, through which the wave propagates, adds a third acoustic impedance which is undetermined. This could allow complete reflection at the interface if the coupling were extremely poor. A poor couplant in conjunction with an angle of incidence slightly different from perpendicular can cause the mysterious disappearance of a shear wave which existed strongly at the boundary of the first media and cause it to be replaced by a longitudinal wave sensed at the end of the second media.

In addition to the problem of control of the mode conversion, reflection, and coupling of an ultrasonic wave, a more intense wave must be generated so that it may penetrate a thick lossy material.
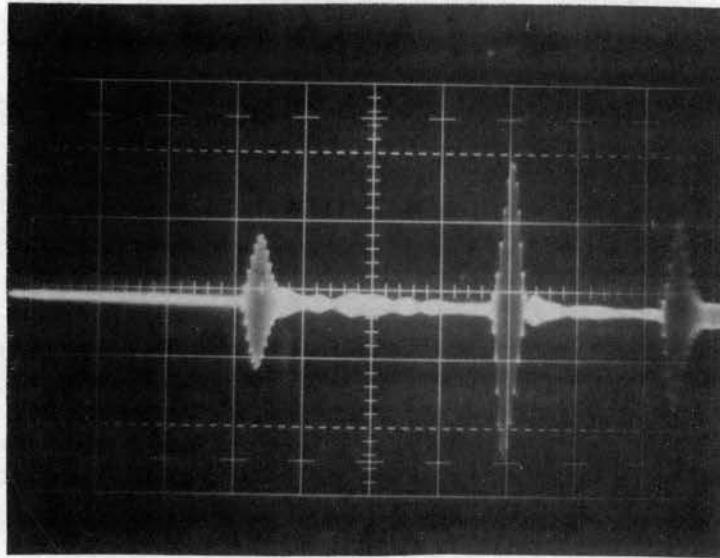
Figure 9. Buffer Block Signal with Reflections
Dispersed by Scattering.

CHAPTER IV

THE DESIGN OF AN ELECTRO-ACOUSTIC GENERATOR FOR THE

GENERATION OF HIGH INTENSITY WAVES

In ultrasonic testing methods the type of pulse applied to the send-
ing transducer limits the use of the testing machine. The most desirable
pulse for the method used in materials testing is a gated sine wave. The
gated sine wave driving a crystal can correspond to a natural frequency
of the crystal, thus driving the crystal in the most efficient manner.
Typical response oscillograms showing the difference in crystal response
to a pulse versus a gated sine wave can be found in most ultrasonics texts.
If the pulse width (time duration of the pulse) is variable from 1 to 15
microseconds, the generated acoustic wave will be more usable than if a
long duration pulse existed. For example, if the time necessary for a
shear wave to propagate through a metal is 2 microseconds and there is
mode conversion at the first interface (both shear and longitudinal waves
generated simultaneously), the longitudinal wave would take approximately
1 microsecond to traverse the material since a shear wave travels approxi-
mately half as fast as a longitudinal wave in metals. The pulse length
would necessarily be less than 1 microsecond if the two waves are to be
distinguished.

A piezoelectric crystal system used to generate an acoustic wave
consists of an electrical inductor-capacitor circuit. When pulsed, the

circuit oscillates at its natural frequency until the energy is dissipated. Control of the pulse length or time duration of oscillation requires some means of controlling the oscillation of the crystal system.

A series or parallel resistance will lower the circuit Q and essentially reduce the circuit ring time, but this produces a pulse whose amplitude decays exponentially. The desired gated pulse must fall in amplitude in negligible time. Arenberg uses an electronic damping circuit in his Model PG 650 pulsed oscillator, which is manufactured by Arenberg Ultrasonic Laboratories. This circuit consists of a diode connected to the output of the pulser. The diode has its cathode biased to a high voltage for the desired period of time to allow the sine oscillation to drive the crystal circuit. At the end of the pulse the bias is removed from the diode, and the cathode is then essentially grounded. This situation then grounds the oscillating circuit and immediately the oscillation ceases.

When quartz crystals are used, an extremely high voltage is necessary to drive the high impednace crystals; i.e., to drive the relatively inefficient quartz crystals to produce a high intensity acoustic wave, a high power input is necessary. In order to drive the high impedance crystal at a high power level, an extremely high voltage is necessary since $P = V^2/Z$.

Maximum power transfer from the driving oscillator to the quartz crystal requires that the load impedance (crystal) be closely matched to the output impedance of the oscillator.

A quartz crystal which has a fundamental natural frequency of 500 kilocycles per second has an impedance on the order of one megohm

(depending on size). The output impedance (plate-to-plate) of a power oscillator may be 5000 ohms. The impedance mismatch between the oscillator and a quartz crystal of approximately one megohm impedance allows only a small portion of the oscillator power level to reach the crystal. At frequencies below one megacycle an impedance transformer can be used without excessive power loss (ferrite core). Above one megacycle an air core transformer is usually necessary.

If the quartz crystal is remotely located, a transformation to a low impedance line is necessary. The highest impedance coaxial cable is about 600 ohms. This cable consists of an external conductor (shield) of copper tubing with a diameter of several inches containing a center conductor which is a tightly stretched wire. Since a value of 600 ohms would be an upper bound, the difference between available cables (commercial) and a constructed high impedance cable is not significant in the general case. The typical commercial cable is 50 or 75 ohms in characteristic impedance. The output impedance of the power generator must be transformed to the 75 ohm coaxial cable, and then the 75 ohm cable must be matched to the high impedance of the crystal. Impedance matching of this type is accomplished by air core transformers. The network must be carefully matched to the two driving crystals. The circuits used in the air core transformers are tuned resonant circuits each mutually coupled inductively. The time necessary for the tuned circuits to rise to maximum voltage is affected by the degree of coupling, and the time duration necessary for the cessation of oscillation depends upon the Q of the circuit. Therefore, a true gated sine wave is impossible to transmit to

the quartz crystals. The gated sine wave condition can be approached as the operation frequency increases.

Even when a true gated sine wave is applied to a quartz crystal, it will not produce an acoustic wave with the same shape as the driving volt-age unless the crystal is highly damped. This is the damping that results from the physical attachment of the front face of the crystal to a buffer block and loading of the back face so that it cannot reflect energy. Receiving crystals are not as sensitive to damping as the driving crystals since the received energy is not as great as the driving energy.

By incorporating an electronically damped gated oscillator and by matching the impedance of the driven piezoelectric crystals to the output impedance of the oscillator, an electrical pulse with a fast rise and fall time can be applied to the piezoelectric crystals. A fast-rise, fast-fall acoustic pulse with an almost rectangular shape can be generated if the electrical pulse is applied to a highly damped piezoelectric crystal.

The crystals are damped by firm attachment to the buffer blocks with Eastman 910 cement or similar cements with higher temperature capabilities. The crystal must be backed with a material closely matching the acoustic impedance of the quartz. This would allow the generated wave to pass into the backing material and then be damped or at least separated in time sequence so that it would not disturb the desired signals. A sub-stitute here would be a thick layer of silicone vacuum grease to absorb and thus reduce the back face reflections of the crystal.

Sufficient power must be available from the oscillator to drive the quartz crystals. With an unlimited power capability in the oscillator, the energy level of the generated acoustic wave is limited by the thickness

of the crystal. The crystal limits the power level since arcing would occur when the voltage reaches a sufficiently high level.

The selection of oscillator power tubes with sufficient power output and careful impedance matching allows the generation of acoustic waves of sufficient amplitude to traverse the urethane samples and remain readable. This satisfies the condition of being able to test highly damped materials as posed in the original statement of the problem.

A description of the design and construction of the circuit follows.

The Power Oscillator

The output stage of the pulse packet generator was chosen to be a push-pull system of either tetrode or pentode tubes. The reasons for this choice were:

1. The push-pull system could be easily stopped from oscillation by removal of screen voltage.

2. Power output could easily be varied by adjustment of plate and/or screen voltage.

3. The availability of a large selection of tubes would make possible various maximum power capabilities.

4. The output impedance of the power oscillator could be selected by choosing different tetrodes or pentodes.

5. The build-up time of oscillation is extremely short since the circuit resembles the Eccles-Jordan flip-flop circuit. This creates a fast rise time on the envelope of the pulse packet.

6. The power necessary to drive the grids of the output tubes is negligible.

The output stage operates in a balanced push-pull manner with each tube driving the other in a manner similar to the Eccles-Jordan flip-flop. The frequency of oscillation was determined by a tuned circuit using a variable capacitor in parallel with the primary of the output transformer (air core). The output wave form is a sine wave since the load is a tuned circuit. The oscillation of the output stage is started and stopped by gating both the control grids and the screen grids of both tubes simultaneously. The cathodes of each tube are biased by a common cathode resistor requiring each tube to have a zero or negative voltage with respect to the cathode on both the grid and screen until gated. A suitable gating voltage is then applied to both the control grids and screens, and oscillation immediately starts. When the gating voltage is removed, the tubes cease oscillation immediately since the screen voltage is zero or negative rendering the tube efficiency to a zero value. The grids can still be driven positive by the tank circuit oscillation, but the tubes do not conduct since the screen voltage is negligible. The circuit is shown in Figure 10.

The gating voltage applied to the screen grids and control grids can be from the same source if an isolation resistor is placed between the grids and screens as is shown dashed in Figure 10. Although the tank circuit can now drive the screens, no oscillation can continue because the tank circuit cannot drive the screen grids sufficiently positive to allow the continuation of oscillation when the gating voltage is removed.

When the output is operated unbalanced, extreme parasitic oscillation suppresion must be employed to prevent ultra-high frequency oscillation. Parasitic suppressors wound on the plate resistors should be used

Output

B$^+$

Tank Circuit
Which Determines
Oscillation
Frequency

Screen
Gating
Voltage

Grounded
or
Biased
Above
Ground

Grid Gating
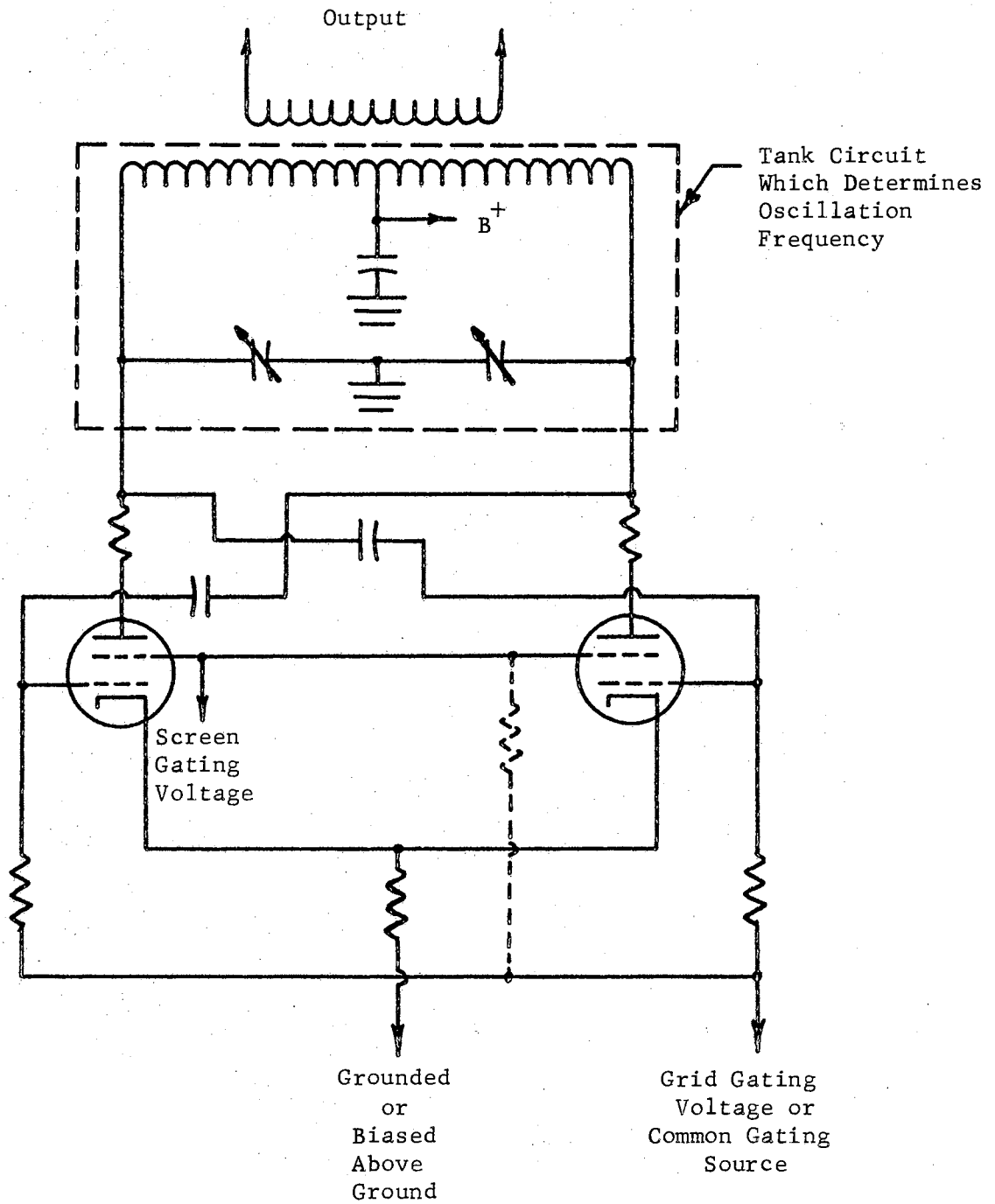Voltage or
Common Gating
Source

Figure 10. Basic Oscillator Circuit.

regardless of the type of output. Short leads from the output tube plates

to the tank circuit are necessary, and symmetrical physical location also

aids to prevent parasitic oscillation.

The reason that the unbalanced operation of the output (one side

grounded) can cause parasitic oscillation is that the distributed capaci-

tance of the coils with respect to the chassis ground on each half of the

output transformer is no longer balanced. The situation is described in

Figure 11. The unbalanced situation in each half of the tuned circuit

in the output stage would require that two or more oscillation frequencies

exist. This leads to an unstable situation and requires considerable

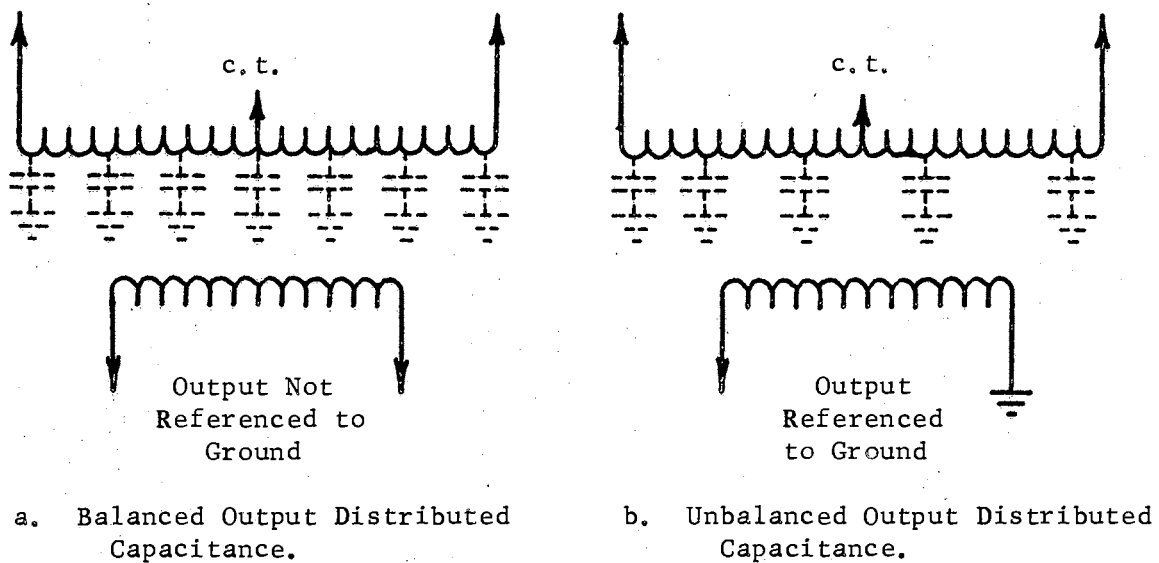precautions to assure single frequency oscillation.

a. Balanced Output Distributed Capacitance.

b. Unbalanced Output Distributed Capacitance.

Figure 11. Balanced and Unbalanced Transformer Operation.

Impedance Matching

The impedance match between the plate-to-plate impedance of the output oscillator and the quartz crystals was accomplished by air-core transformation. Figure 12 shows a schematic of the system.

The impedance network of part a, Figure 12 has a low impedance link which allows the crystal to be located a distance from the power oscillator. The allowable length of the link would be limited by the frequency of operation. The length of the link should be less than a quarter wave length to insure that excessive radiation losses do not occur.

The impedance matching network of part b, Figure 12, is commonly used for pulsed oscillators. It has disadvantages in that the tuning of the output circuit driving the crystal is accomplished by balancing the capacitance of the crystal, the capacitance of the wire, and the capacitance between turns of the output transformer with the inductance of the transformer. Often the tuning is accomplished by varying the length of connecting wires. Any frequency change would then require changes in coupling wire. The system almost requires unbalanced operation as most systems automatically ground one side of the line. Extremely high Q values usually result which makes tuning difficult. This is especially true for pulse-echo work. It should be noted that this type of network would suggest that high impedance (plate-to-plate) output tubes would be required if the system were to drive high impedance quartz crystals. This would allow the transformer to approach a one to one ratio of impedance transformation. A high impedance tube requires a high voltage plate supply if sufficient power is to be generated, and this also requires high voltage components in the output stage.
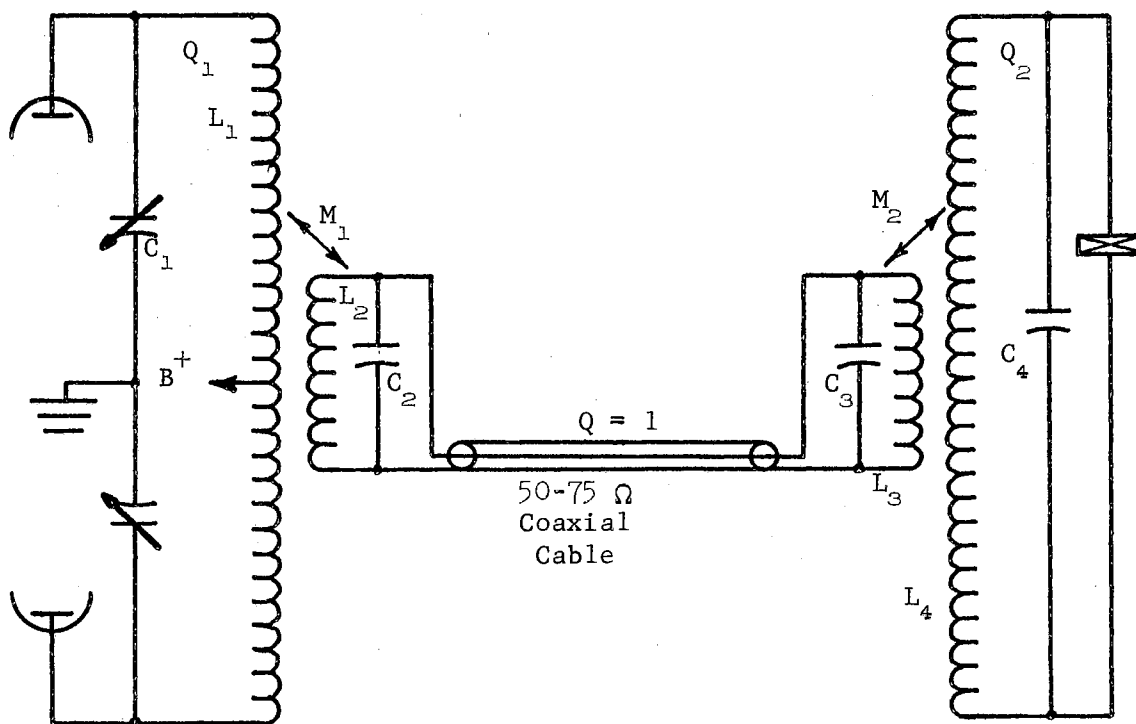
a. Impedance Matching Network with Shielded
   Transmission Link.
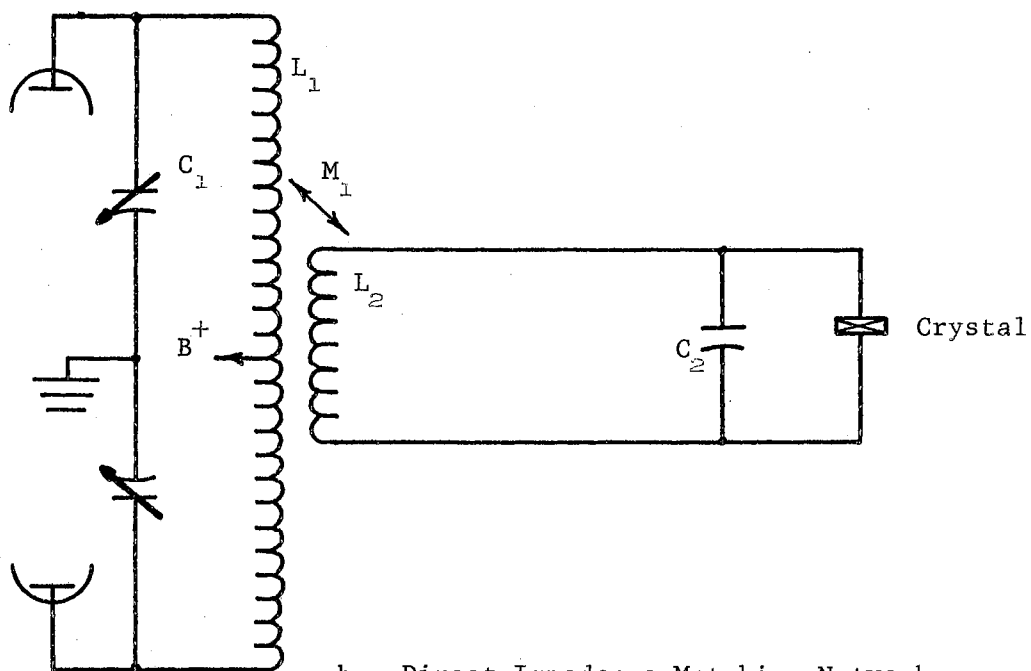
b. Direct Impedance Matching Network.

Figure 12. Impedance Matching Networks.

The impedance matching network of Part a, Figure 12, would suggest the use of output tubes with low plate-to-plate impedance. This would lower the impedance transformation necessary to match the 50 to 75 ohm link line. The low impedance tubes (plate-to-plate) are low plate voltage, high current tubes which then would not require such high voltage components. The link line length can be increased without detuning the network.

Design Procedure

The quartz crystals were mounted on a buffer block and the reactance and resistive components of the impedance were found by using a Q-meter. The design of the impedance matching network shown in Part a, Figure 12, was done following the standard Q-equation methods. Using the relationships derived for the design of the network, all values of inductance, capacitance, mutual coupling, and Q were either calculated or chosen. The coils L_1, L_2, L_3, and L_4 were then wound. The inductance of each was set at the calculated value using a standard 1000 cps impedance bridge. A number of capacitors was checked with the impedance bridge until a suitable capacitance value was found.

The impedance network was then assembled and tested. The first network tried was for the 500,000 cps crystals. The network was the most efficient at a frequency far below 500,000 cps. The system was useless at 500,000 cps. The network was then analyzed and the trouble isolated. It was found that the coil L_4 had a resonance point at the frequency corresponding to the most efficient frequency of the network. This coil resonance occurred because the inductance of the coil in conjunction with

the capacitance between the turns of the coil formed its own tuned circuit. The coil size (inductance) had to be reduced until the natural resonance of L_4 was above the natural frequency of the crystals. This problem arises in all coils, but theoretical derivations on impedance networks do not mention the fact. The decrease in L_4 required an increase in C_4 which raised the Q of that part of the circuit. This was undesirable in that it increased ring time and made the tuning necessarily very precise.

The problem here consisted of two parts. First, capacitance in the coil L_4 prevented the use of desired Q values. Second, the Q equations were correct, but it is physically impossible to obtain a pure inductance or capacitance. This caused the difference in performance between the actual network and that predicted by the Q equations.

The best solution to the impedance matching problem was to use the Q equations to get approximate values. A step-by-step procedure follows:

Step 1. A suitable dual section variable capacitor (C_1) must be selected. The size coil (L_1) necessary to resonate with the variable capacitor must be calculated. Sufficient accuracy of the coil can be obtained by measuring the inductance with an impedance bridge. The Q of the circuit (Q_1) should be controlled to allow easy tuning and realizable coupling coefficients. The variable capacitor will allow wide variations in coil size to control the value Q_1.

Step 2. A link coaxial cable of 50 or 75 ohms characteristic impedance must be selected. The values of L_2, C_2, L_3, and C_3 must be determined by calculation so that the Q will be one. In actuality, capacitors C_2 and C_3 should be selected bearing the capacitance values calculated

to produce a Q of one. Then, coil L_2 should be wound so that its
inductance at 1000 cps coincides with the calculated value necessary to
produce a Q of one. Coil L_3 must be wound larger in inductance than
L_2 and attached. Inductively an oscillator (sine wave) must be coupled
to the link coil by winding a few turns of wire into a coil and attaching
the ends of the wire to the oscillator. The coil from the oscillator
must be placed close to the coil L_2. The high impedance probe of an
oscilloscope must be attached across L_2. The frequency of the oscillator
must be adjusted to the desired operating frequency, and the coil L_3 must
be unwound until the voltage (oscilloscope) peaks at the desired frequency.
The oscillator frequency must be varied to be certain that the circuit
contains no resonant frequencies below the desired operating frequency.

Step 3. The quartz crystals must be mounted and suitable leads
attached. Basic calculations must be made to determine the necessary
values of L_4 and C_4 to produce a given value of Q_2 to produce the
impedance match necessary for the crystal and still be able to wind a
coil which will not itself resonate below the desired operating frequency.
At low frequencies the coil size may prevent exact impedance matching.
Usually the crystal itself will have sufficient capacitance C_4. If not,
the calculated value of C_4 can be inserted, and L_4 is then wound so
that its inductance is greater than the necessary calculated value. The
coil connected to the oscillator is then positioned near L_4 (coupled).
The oscilloscope probe is attached across L_4, and the oscillator is then
adjusted to the desired operating frequency. L_4 is then unwound until
maximum voltage occurs across L_4. The oscillator frequency is then
varied to be certain that no resonant peaks occur below the desired

operating frequency. The circuit should then be connected together, and the coupling between L_1 and L_2 adjusted for maximum voltage across L_4. Then the coupling between L_3 and L_4 should be adjusted for maximum voltage across L_4. The capacitor C_1 should then be varied about the desired operating frequency to check if the circuit has maximum voltage across L_4 at the desired operating frequency. If it does not then L_4 should be varied until the maximum voltage across L_4 occurs at the desired operating frequency. Multiple voltage peaks close to the desired operating frequency indicate that the link circuit and L_4--C_4 are not tuned at the same frequency. This occurs because of the change in inductance from mutual coupling.

It should be noted that this network matches the oscillator impedance to specific crystals (impedance). This means that a universal machine of this nature is questionable when it is to have several different crystals attached. An impedance network would be required for each crystal.

Pulse Shaping

The power oscillator is capable of generating a gated sine wave which has essentially a square envelope. The application of the gating voltage starts the oscillation and removal of the voltage causes immediate cessation of the oscillation of the tubes. The tuned circuit containing L_1 and C_1 can still oscillate until its energy dissipates. The same situation exists in the circuit containing L_4 and C_4. The power oscillator begins oscillation and reaches maximum in negligible time, and nothing more can be done to improve the rise time of the wave packet applied to the crystals and still have proper impedance matching. When the oscillator

ceases, each part of the circuit will ring for about $Q/3$ cycles. This does not then produce a square wave packet. To reduce the decay or fall time of the wave packet, two diodes need to be introduced into the circuit as shown in Figure 13.

The gating pulse applied to the control grids and screen grids of the output tubes is also applied to the cathodes of the diodes preventing any conduction as the cathodes are essentially at the same voltage as the plates. When the gating voltage is removed, the oscillator tubes cease ososcillation and the cathodes of the two diodes then approach ground potential as far as any alternating voltage is concerned. The voltages in the tank circuit containing C_1 and L_1 then cause conduction through the two diodes. This causes immediate cessation of oscillation in the tank circuit.
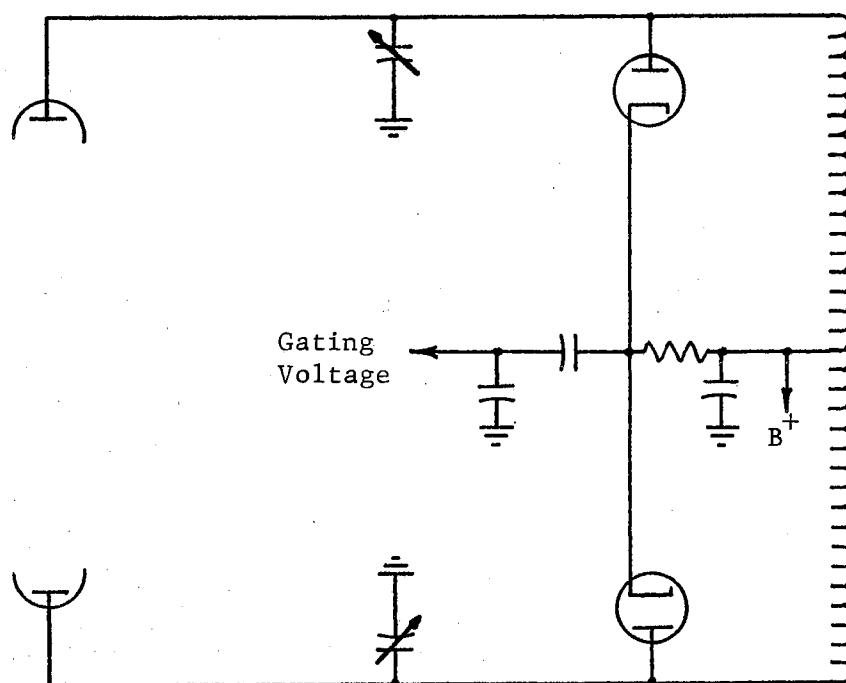
Figure 13.   Diode Damping

The procedures described provide a pulse packet with relatively fast rise and fall times. The correct impedance match allows peak-to-peak voltages to be applied to the crystals in excess of 4000 volts when two 6146 tubes are used. Plate voltage on the 6146 tubes should be kept below 600 volts to control the applied crystal voltage so arc-over will not occur. The system is capable of generating ultrasonic waves of high intensity which are needed to penetrate a lossy material.

CHAPTER V

EXPERIMENTAL DATA

A series of laboratory samples of urethanes was acquired for test

purposes to prove the capability of the machine to test lossy materials.

The urethanes were formulated by mixing different proportions of two

urethanes developed by Dow Chemical. The formulations and some data on

them are given in Table II. The different formulations of the urethanes

produced a series of urethanes possessing widely separated properties.

These urethanes possessed densities that encompassed the densities of the

urethanes used in a paper by H. E. Van Valkenburg, A. M. Murdock, and P.

Kraynak entitled "Ultrasonic Properties of Solid Propellant Binders" [the

work was done at Sperry Products under Air Force Contract AF 33(616)-

7069]. This paper stated that,

> At test frequencies of 1 mc and higher no shear wave trans-
> mission could be detected above -10°C due to the extremely high
> attenuation. Data points below -40°C tended to be erratic due
> possibly to formation of ice crystals and couplant sludge.

The usual ultrasonic test methods use either immersion techniques

or a cementing of the test sample to the buffer blocks. One of the pur-

poses of the test method developed in this study was to further the state

of the art by being able to test a sample of urethane without a cement

type couplant and to test at room temperature at 2.25 megacycles (above

that deemed possible in the quoted article). The selected couplant was

20 weight motor oil.

TABLE II

URETHANE SAMPLE DATA FURNISHED BY SUPPLIER

Formulations and Physical Properties of

Polyether Urethane Elastomers

Formulation Number	Parts By Weight				Density (g/cc)	Durometer (Wallace)	Initial (x 10^{-4}) Modulus (psi)
	CP-700	P-2000	TDI	Catalyst			
100	100	--	40.2	.1	1.134	91.5	7.420
85-15	85	15	35.5	.1	1.121	71.7	1.688
70-30	70	30	30.9	.1	1.109	68.6	1.466
55-45	55	45	26.2	.1	1.093	66.1	1.324
40-60	40	60	21.5	.1	1.065	58.6	.965
25-75	25	75	16.9	.1	1.054	54.5	.787

The data on the urethane samples furnished by the supplier appears
in Table II. It should be noted that the data obtained ultrasonically
was basically determined by the measurement of the time required for the
wave to traverse the test sample. This time could be read to the nearest
$\frac{1}{8}$ microsecond in the worst possible case. The scatter of data from
repeated tests was extremely small.

The test data on the urethane samples was intended to prove the capa-
bility of testing the samples. This required that an ultrasonic wave of
sufficient intensity be generated and suitably coupled to a sample to
produce a readable wave at the opposite side of the sample. The suggested
test method using a two-path interferometer would yield data more accurate
than that tabulated in Table III. The accuracy of the suggested test
system has already been established. The problem was to be able to obtain
test data which requires that a readable shear wave penetrate the sample.
For this reason all efforts were concentrated on being able to produce an
ultrasonic wave of sufficient amplitude to be detected. The test data
obtained was intended to prove only that a readable wave was produced.
Therefore, only a single acoustic path was used. The dual path system
suggested will certainly operate if a single path system operates.

The accuracy of the calculated data in Table III is unknown; however,
the repeatability of the data obtained was excellent. A survey of litera-
ture showed that similar single-path test methods used on less challenging
test materials yielded results whose accuracy was within 20%. A discus-
sion of the error in moduli due to measurement error appears in Appendix B.

The testing procedure used to determine the data of Table III was to
place the receiving crystal on the end of the buffer block and establish

TABLE III

CALCULATED WAVE VELOCITY, ATTENUATION, AND COMPLEX MODULI FOR URETHANES

Formulation (See Table 2)	URETHANES Temperature 80° ± 2°F				
	Velocity				$\bar{E} = E + j\omega E'$
	V_ℓ in/sec	V_ℓ cm/sec	V_s in/sec	V_s cm/sec	E lb/in²
100-0	89,100	226,000	34,600	87,900	8.33×10^5
85-15	80,000	203,000	32,000	81,700	6.66×10^5
70-30	69,300	176,000	29,300	74,400	4.91×10^5
55-45	63,200	161,000	26,300	66,800	4.04×10^5
40-60	56,700	142,000	26,000	66,000	3.14×10^5
25-75	56,100	143,000	25,700	62,700	3.07×10^5
	Attenuation				$\omega E'$ lb/in²
	Shear Wave		Longitudinal Wave		
	db/in	nep./cm	db/in	nep./cm	
100-0	150	6.84	75	3.41	10,730
85-15	198	8.97	128	5.80	11,100
70-30	205	9.32	120	5.44	8,660
55-45	246	11.2	111	5.03	7,450
40-60	233	10.5	193	8.70	9,250
25-75	173	7.84	142	6.42	4,510

a time reference on the oscilloscope. Then the test sample was inserted and readings of time delay on the wave and relative amplitude of the wave were taken for both longitudinal and shear waves.

The oscillograms in Appendix C prove the existence of longitudinal and shear waves emerging from the test samples.

A series of rubbers, a plastic, and selected metals were also tested, and the oscilloscope trace pictures for some of these also appear in Appendix C. These pictures prove the existence of longitudinal and shear waves at the sample boundary opposite the buffer block.

The maximum strain occurring as the stress wave travels through the urethane was small. Therefore, the modulus associated with the strain wave would approach the initial modulus. The initial modulus of elasticity tabulated in Table II was derived by drawing a tangent line at the origin of the stress-strain curve. The material was strained three times, and the third stress-strain curve was used to obtain the data. Since the slope of the tangent line corresponds to the stress-strain curve only at the origin, it determines properties which are accurate only when the strain is small (approaching zero).

The standard tensile test will yield different property values if the rate of straining is changed. A dynamic test using the resonance method may determine property values which differ from values obtained by a tensile tester. Any test method obtains data which is relative. However, the standard of performance of a material in service can be determined by experiment. Then, the material along with other materials can be tested by a single test method, and the relative performance of the materials in service can be predicted. If different property values could

not be obtained under different testing conditions, no "standard" test methods would be available. It is expected that different test methods will yield different values of properties.

The attenuation values of the different formulations of urethane shown in Table III do not vary proportionately with change of formulation. Although the actual value of attenuation is in question, the variation in attenuation values for different formulations suggests inaccuracy in the measurement of wave attenuation.

An insight into the inaccuracies of the attenuation values was obtained through experimentation with different buffer blocks. Buffer blocks made from the same material but with their ends having different degrees of parallelism were used. Until the two ends approached parallelism, no shear wave could be detected by the receiving crystal when the test sample was inserted. The ends of the buffer blocks were slightly crowned which limited the usable area. The loss of wave energy due to differences in coupling and location of the receiving crystal (which was larger in area than the usable area of the buffer block) caused the error in attenuation values. The error in attenuation values could be minimized by manufacturing buffer blocks with flat, parallel ends. The error arising from different degrees of coupling cannot be predicted even if cements are used for attachment. Silicon vacuum grease was substituted for the oil couplant with the result of slightly higher attenuation readings. This was done to prove that the test method would work with the grease. Vacuum grease is stable over a wide temperature range.

The modulus values obtained by the ultrasonic method were on the order of ten times higher than those furnished by the supplier of the

urethanes. As a check on the accuracy of the order of magnitude, a 1.00

inch thick aluminum sample was tested, and the modulus value was deter-

mined to be 15.5 x 10^6 psi as opposed to 15.8 x 10^6 psi obtained from

handbook data. Since the data was repeatable, it was assumed that the

order of magnitude of the moduli was correct. It should be noted that

the strain associated with an ultrasonic wave is small. This is essen-

tially approaching a limiting condition of zero strain. The modulus

values would approach a maximum theoretical value in a manner analagous

to the strength of a fiber approaching theoretical strengths of atom

separation.

The horizontal time scale of the oscilloscope was set at 10 micro-

seconds per centimeter in order to determine the velocity of a shear

wave. The reference oscillogram (Part a, Figure 14) was otabined by

placing the receiving transducer directly on the end of the buffer block.

The first longitudinal wave designated by the "Longitudinal Wave" arrow

occurs at 29 microseconds. The shear wave identified by the "Shear Wave"

arrow appears at 65 microseconds. The receiving transducer is removed,

and the test sample is inserted between the buffer block and the receiv-

ing crystal. The resulting oscillogram (Part b, Figure 14) now shows the

"Longitudinal Wave" to appear at approximately 32 microseconds. It should

be noted that all time measurements are taken from the initial portion of

the wave. The difference in the two readings is 32 - 29 = 3 microseconds.

This must be the time necessary for the longitudinal wave to traverse the

sample. The sample thickness is 0.159 inches thick; therefore, the veloc-

ity of the longitudinal wave is 0.159/3 x 10^{-6}. The time of travel of

the longitudinal wave has now been determined to be 3 microseconds. The
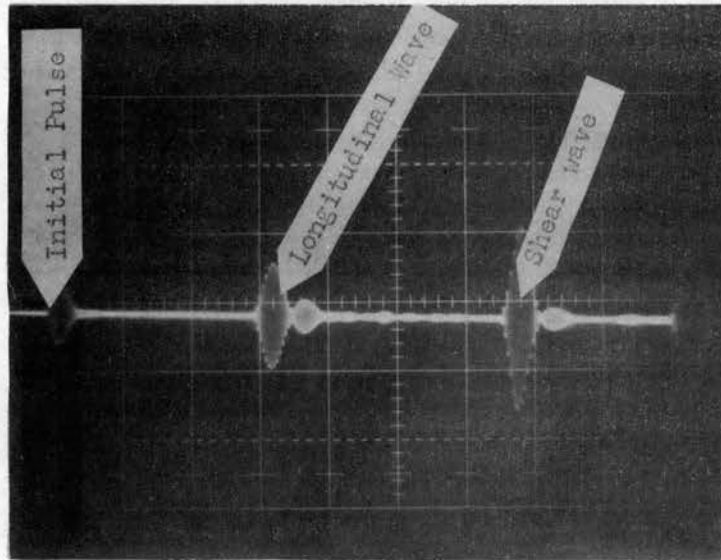
Part a. 85-15 Formulation Urethane Reference
.01 v/cm.
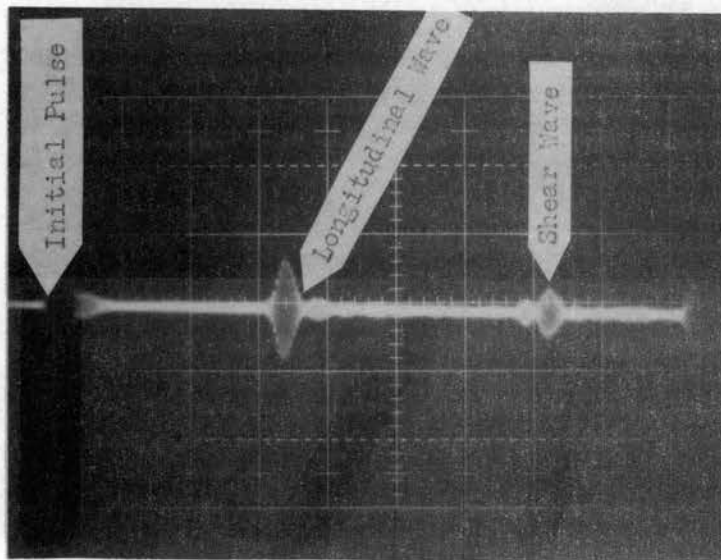
Part b. 85-15 Formulation Urethane 0.001 v/cm.

Figure 14. Shear Wave Velocity Measurements.

shear wave travels approximately half as fast as the longitudinal wave.

This would then require 6 microseconds. The shear wave should appear at

65 + 6 or 71 microseconds. This wave is denoted by the "Shear Wave"

arrow on Part b of Figure 14. This reading is closer to 70 microseconds;

therefore, the velocity of the shear wave would be $0.159/70 - 65 \times 10^{-6}$

inches per second. The wave located to the left of the shear wave in

Figure 14, Part b should be noted. It is the longitudinal mode conver-

sion of the shear wave which impinged upon the test sample. Without the

prediction of the shear wave position, there would be no basis for the

decision of which wave should be used. The wave in Figure 14, Part b,

designated by the "Shear Wave" arrow cannot be a longitudinal wave reflec-

tion as the next possible position of a reflected longitudinal wave would

be at 65 + (3) (3) = 74 microseconds.

CHAPTER VI

CONCLUSIONS AND RECOMMENDATIONS

An ultrasonic method of testing lossy materials (urethane) at room temperature and at 2.25 megacycles was developed. The method was capable of testing urethane under conditions well outside previous limits. It extended the ultrasonic testing field so that the behavior of many lossy materials can now be determined at higher temperatures than was heretofore possible.

The specific contribution of this work is the development of a high power electronic pulsed-oscillator capable of driving a high impedance crystal remotely located from the generator. Also, an orginal system of interpreting ultrasonic wave reflections is presented which can definitely prove the identity of a shear wave traversing the test sample. This differentiates this test method from any other found in literature; thus, it represents a new technique in testing.

The test method developed is capable of testing lossy materials under more difficult conditions because of the following reasons:

1. A method of developing a high intensity shear wave was devised. The intensity of the 2.25 megacycle per second shear wave is sufficient to penetrate urethane samples 0.156 inch in thickness at room temperature (80°F), thus making testing possible.

First, the generation of a high intensity wave was possible because a pulsed oscillator of high power output (over 100 watts continuous) was used. Second, an impedance matching network was devised (along with a step-by-step construction procedure) so that the available power could be delivered with minimum loss to the quartz transmitting crystals. Third, the transmitting crystals were secured to the buffer blocks by Eastman 910 cement allowing the higher degree of coupling necessary to transmit the high intensity wave generated by the crystal. A thick layer of silicone vacuum grease was placed over the back of the Y-cut quartz crystal to load the back face and also to help prevent arc-over. The firm attachment of the crystal along with the back face loading allowed the crystal to vibrate in a manner that closely followed the variation of the electrical voltage applied.

2. A unique interpretation procedure was developed to aid in locating a low amplitude (highly damped) shear wave detected by the receiving crystal.

The interpretation procedure consisted of first determining the longitudinal wave transit time and then assuming that the shear wave transit time was twice that value. This assumption is not correct but when the sample thickness is 0.156 inches, the assumption is sufficiently accurate to predict the time position of the shear wave. The transit time of the longitudinal wave was used to determine the time position of all reflected longitudinal waves. This information made possible the indentification of the received shear wave. It should be noted that a shear

wave crystal generates simultaneously both longitudinal and shear waves.

The receiving crystals were directly coupled to the test sample (no buffer blocks) so that additional reflections within buffer blocks would not complicate the interpretation procedure.

Buffer blocks were used between the transmitting crystal and the test sample to time separate the simultaneously generated longitudinal and shear waves. The length of the buffer blocks was sufficient to prevent longitudinal wave reflections from within the buffer blocks from becoming coincident with the slower traveling shear wave.

3. The problem of mode conversion of the shear wave at the buffer block-sample interface was analyzed, and the construction of the buffer block was altered to determine a method of minimizing the mode conversion. It was determined that mode conversion at the interface was due to unparallel and non-plane faces of the buffer block. Either case allowed the existence of two wave modes (longitudinal and shear) in the test sample with each mode obeying Snell's law of refraction. This allows the systematic solution of the mode conversion problem at a buffer block-sample interface. The acoustic impedance mismatch resulting from poor coupling between the buffer block and the test sample can also deter the propagation of a shear wave into the test sample. In problem cases the exact cause should be determined so that a proper solution can be found. A cement type coupling as opposed to oil should be used first. If a considerable improvement is

not observed, then the problem is definitely the geometry of the buffer block.

General Observations

1. The thickness of the test sample (highly damped) should be as large as possible yet still allow penetration by the ultrasonic wave. This improves the sample thickness to couplant thickness ratio and insures that the testing results apply to the material and not to the coupling medium. Also, a thicker sample can be measured (physical size) with higher accuracy.

2. The time delay resulting from wave travel through the test sample dictates the necessary time separation between the longitudinal and shear waves in the buffer block. Thus, the buffer block length and sample thickness are related. This fact must be considered in test machine design.

3. A two path interferometer test machine with different sample thickness in each path should be used to increase the accuracy of attenuation measurements. This method reduces the error in attenuation measurements resulting from wave reflection and mode conversion at interfaces.

The test method and allied equipment developed in this study allow the study of material behavior outside the present test limits. For example, the variation of the modulus of elasticity of certain materials can now be studied over a wider range of temperature. The internal damping of certain materials can also be studied in new areas of testing. This allows a better prediction of the material's behavior under load. In formulating new materials, more can now be learned of the effects of small changes in material composition.

The specific problems which were confronted in this study point out a need for further study in several areas. The first area would be to develop electronic gear capable of delivering still higher peak powers to high impedance crystals. The second area would be to study the adaptability of suitable backing or damping materials for quartz crystals. The backing material must be capable of withstanding 500°F. Third, a study should be made on the limits of accuracy of machining buffer blocks. This would include the flatness of the ends along with the degree of being parallel. A systematic study should be made of the effects produced by small variations in flatness and parallelism. Also, it is suggested that a silicon-controlled rectifier be added to the link line of the impedance matching network, and that it be triggered into conduction at the end of each pulse. This would help to damp oscillations in the system and allow a faster fall time of the pulse. In summary, the recommendations noted here would allow even further study into the behavior of difficult materials.

SELECTED BIBLIOGRAPHY

Books

1. Bergen, J. T., ed., _Viscoelasticity_, Academic Press, New York, 1960.

2. Ewing, W. M., W. S. Jardetsky, and F. Press, _Elastic Waves in Layered Media_, McGraw-Hill, New York, n.d.

3. Ferry, J. D., _Viscoelastic Properties of Polymers_, John Wiley and Sons, New York, 1961.

4. Kolsky, H., "Mechanical Testing of High Polymers," _Progress in NDT_, Vol. 2, ed. by Stanford and Fearon, MacMillan, New York, 1960.

5. Kolsky, H., _Stress Waves in Solids_, Oxford, 1953.

6. Krautkramer, J., and H. Krautkramer, _Werkstoffprofung Mit Ultraschall_, Springer, Berlin, 1961.

7. Love, A. E. H., _The Mathematical Theory of Elasticity_, 4th Ed., (1st American Ed.), University Press, Cambridge, 1944.

8. McGonnagle, W. J., _Nondestructive Testing_, McGraw-Hill, New York, 1961.

9. Mason, W. P., _Physical Acoustics and the Properties of Solids_, Van Nostrand, 1958.

10. Morse, P. M., _Vibration and Sound_, McGraw-Hill, New York, 1948.

11. Sokolnikoff, I. S., _The Mathematical Theory of Elasticity_, McGraw-Hill, New York, 1946.

12. Sommerfield, A., _Mechanics of Deformable Bodies_, Academic Press, New York, 1950.

13. Stephens, A. W. B., "Application of Damping Capacity of Investigating the Structure of Solids," _Progress in NDT_, Vol. 1, MacMillan, New York, 1959.

Articles

1. ASTM Symposium on Dynamic Stress Determination, San Francisco, 1949, Publication STP 104, American Society for Testing Materials, Philadelphia, 1950.

2. ASTM Symposium on Determination of Elastic Constants, 1952, Publication STP 129, American Society for Testing Materials, Philadelphia, 1952.

3. Bancroft, D., "The Velocity of Longitudinal Waves in Cylindrical Bars," Phys. Rev. 59, 1941, pp. 588-593.

4. Beltner, A. A., "Special Research Bibliography--Physics of Ultrasonics and Hypersonics in Solids," Missile and Space Division, Lockheed Aircraft, SRB-60-9, September, 1960.

5. Bergmann, L., der Ultraschall, Bibliography, Edition 6 (includes 5000 references), 1954; Supplemental Bibliography (includes 200 additional references), 1957.

6. Boor, L., M. Hanok, F. Conant and W. Scoville, Jr., "Rheological Testing of Elastomers at Low Temperatures," ASTM Bulletin, May, 1960, p. 25.

7. Cunningham, J. R. and D. G. Ivey, "Dynamic Properties of Various Rubbers at High Frequencies," Journal of Applied Physics, Vol. 27, No. 9, September, 1956, p. 967.

8. Cusick, J. H., "Nondestructive Testing of Large Solid Propellant Case-Bonded Rocket Motors," Nondestructive Testing, Vol. 18, No. 3, June, 1960, p. 195.

9. Erdman, D. C., "Ultrasonic Tester for JATO Propellant," Electro-Circuits Contract NOas 52-470C (Confidential), Brueau of Aeronautica, 1952-53.

10. Fine, M. E., "Dynamic Methods for Determining the Elastic Constants and Their Temperature Variations in Metals," ASTM Publication STP 129, 1952, p. 43.

11. Gorshkov, N. F., "The Propagation of Pulses in an Elastic Medium With Absorption," Akust. Zh. 3 (Russian), n.d., pp. 154-162.

12. Hastings, C. H., S. A. LoPilato and L. C. Lynnworth, "Ultrasonic Inspection of Reinforced Plastics and Resin--Ceramic Composites," Nondestructive Testing, Vol. 19, No. 5, BMD Contract AF 04(647)-258, September-October, 1961, pp. 340-346.

13. Hatfield, P., "Ultrasonic Measurements on High Polymers," Journal of Applied Physics, Vol. 26, n.d., p. 192.

14. Huter, T., "The Conduction of Ultrasonic Waves in Solid Rods," Z. Agnew. Phys. 1, 1949, pp. 274-289.

15. Kolsky, H., "The Propagation of Stress Pulses in Viscoelastic Solids," Phil. Mag. 1, 1956, pp. 693-710.

16. Kolsky, H., "The Propagation of Stress Waves in Viscoelastic Solids," App. Mech. Rev. 11, 1958, pp. 465-468.

17. Kondrat'ev, A. S. and Z. S. Shaikina, "Oscillatory Properties of the Oscillations of a Longitudinally Compressed Rod," Prikl Mat. I Mekanika 21, 1957, pp. 560-563.

18. McSkimin, H. J., "Measurement of Dynamic Shear Viscosity and Stiffness of Viscous Liquids by Means of Travelling Torsional Waves," J.A.S.A. 24, 1952, pp. 355-365.

19. McSkimin, H. J., "Measurement of Elastic Constants at Low Temperatures by Means of Ultrasonic Waves--Data for Silicon and Germanium Single Crystals, and for Fused Silica," Journal of Applied Physics, Vol. 24, No. 8, August, 1953, p. 988.

20. McSkimin, H. J., "The Propagation of Longitudinal Waves and Shear Waves in Cylindrical Rods at High Frequencies," J.A.S.A. 28, 1959, pp. 484-494.

21. Mapleton, R. A., "Elastic Wave Propagation in Solid Media," Journal of Applied Physics, Vol. 23, 1952, p. 1346.

22. Mason, W. P. and H. J. McSkimin, "Mechanical Properties of Polymers at Ultrasonic Frequencies," Bell System Technical Journal, Vol. 31, No. 1, January, 1952, pp. 122-171.

23. Morse, R. W., "The Velocity of Compressional Waves in Rods of Rectangular Cross Section," J.A.S.A. 22, 1950, pp. 219-223.

24. Murdoch, A. M., "Means for Transmitting and Receiving Ultrasonic Shear Wave Motion," U. S. Paton 2,844,741, July 22, 1958.

25. Naake, H. J. and K. Tamme, "Sound Propagation in Plates and Rods of Rubber-Elastic Materials," Acustica 8, n.d., pp. 65-76.

26. Nolle, A. W., "Methods for Measuring Dynamic Mechanical Properties of Rubber-Like Materials," Journal of Applied Physics, Vol. 19, August, 1948, p. 753.

27. Nolle, A. W., "Longitudinal and Transverse Ultrasonic Waves in a Synthetic Rubber," Journal of Applied Physics, Vol. 23, No. 8, August, 1952, p. 888.

28. Payne, A. R., "Sinusoidal--Strain Dynamic Testing of Rubber Products," Materials Research and Standards, Vol. 1, No. 12, December, 1961, pp. 942-946.

29. Philippoff, W., "Mechanical Investigations of Elastomers in a Wide Range of Frequencies," Journal of Applied Physics, Vol. 24, No. 6, June, 1953, p. 685.

30. Redwood, M. and J. Lamb, "On the Propagation of High Frequency Compressional Waves in Isotropic Cylinders," Proc. Phys. Soc. B 70, 1957, pp. 136-143.

31. Roth, W. and S. R. Rich, "A New Method for Continuous Viscosity Measurement. General Theory of the Ultra-Visconson," Journal of Applied Physics, Vol. w4, No. 7, July, 1953, p. 940.

32. Schneider, W. C. and C. J. Burton, "Determination of the Elastic Constants of Solids by Ultrasonic Methods," Journal of Applied Physics, Vol. 20, January, 1949, p. 48.

33. Schneider, W. C. and C. J. Burton, "Determination of the Elastic Constants of Solids by Ultrasonic Methods," Journal of Applied Physics, Vol. 1, No. 1, January, 1949, pp. 48-58.

34. Schwarzl, F. and A. J. Staverman, "Time-Temperature Dependence of Linear Viscoelastic Behavior," Journal of Applied Physics, Vol. 23, No. 8, August, 1952, p. 838.

35. Shil'krut, D. I., "Velocity of Propagation of Waves in Not Quite Elastic Media," Dokl. Akad. Nauk (Russian), 1956, pp. 58-60.

36. Tahsin, S. I., "Propagation of a Sound Pulse in a Medium with a Complex Modulus," Proc. Iraqi Sci. Socs., Vol. 1, n.d., pp. 1-9.

37. Tiffen, R., "Dilatational and Distortional Vibrations of Semi-Infinite Solids and Plates," Mathermatika, Vol. 3, 1956, pp. 153-163.

38. Truell, R., "References--Propagation of High Frequency Stress Waves in Solids," Draft for Handbuch der Physik, 1962.

39. Williams, J. and J. Lamb, "On the Measurement of Ultrasonic Velocity in Solids," J.A.S.A., Vol. 30, 1958, pp. 308-313.

APPENDIX A

BASIC RELATIONSHIPS FOR MATERIALS

The measurement of the physical properties of a material is accomplished by testing the material to obtain sufficient data to calculate the desired physical properties. In a standard tensile test the force on the sample, the elongation of the sample, and the size of the sample are measured during the test. From this data such properties as modulus of elasticity, Poisson's ratio, bulk modulus, yeidl strength, etc., can be calculated. In an ultrasonic test the wave propagation velocity and the wave attenuation can be determined for several different wave modes.

There must exist some mathematical relationship between the measured data and the desired physical properties. These relationships can be found in any text on the theory of elasticity. Selected mathematical relationships appear in the following paragraphs. These relationships aid in the understanding of the calculation of physical properties.

A material composed of a single crystal possesses properties that are distinct in as many directions as there are distinct directions in the crystal lattice. This means that the strain behavior in the crystal would be described by a tensor which includes the strains in all directions plus the interconnecting terms between strains. In complicated crystals this would require that many directional properties be determined. If a material is composed of a great many crystals, it will probably

possess only one average directional property since the crystals are randomly distributed. The general procedure is to assume the material isotropic and greatly simplify the mathematical relationships necessary to describe the material. This simplification is necessary as a limited number of variables can be measured for a given material.

A three-dimensional isotropic media requires that the mutually perpendicular axes may be translated or rotated and the same conditions still prevail. Otherwise, the material media cannot be isotropic.

Hooke's law must be assumed to be valid in order to mathematically relate stress and strain. With the assumptions mentioned hereto, the following expressions can be derived.

$$\sigma_{xx} = c_{11}\epsilon_{xx} + c_{12}\epsilon_{yy} + c_{13}\epsilon_{zz} + c_{14}\epsilon_{yz} + c_{15}\epsilon_{zx} + c_{16}\epsilon_{xy}$$

$$\sigma_{yy} = c_{21}\epsilon_{xx} + c_{22}\epsilon_{yy} + c_{23}\epsilon_{zz} + c_{24}\epsilon_{yz} + c_{25}\epsilon_{zx} + c_{26}\epsilon_{xy}$$

$$\sigma_{zz} = c_{31}\epsilon_{xx} + c_{32}\epsilon_{yy} + c_{33}\epsilon_{zz} + c_{34}\epsilon_{yz} + c_{35}\epsilon_{zx} + c_{36}\epsilon_{xy}$$

$$\sigma_{yz} = c_{41}\epsilon_{xx} + c_{42}\epsilon_{yy} + c_{43}\epsilon_{zz} + c_{44}\epsilon_{yz} + c_{45}\epsilon_{zx} + c_{46}\epsilon_{xy} \tag{1}$$

$$\sigma_{zx} = c_{51}\epsilon_{xx} + c_{52}\epsilon_{yy} + c_{53}\epsilon_{zz} + c_{54}\epsilon_{yz} + c_{55}\epsilon_{zx} + c_{56}\epsilon_{xy}$$

$$\sigma_{xy} = c_{61}\epsilon_{xx} + c_{62}\epsilon_{yy} + c_{63}\epsilon_{zz} + c_{64}\epsilon_{yz} + c_{65}\epsilon_{zx} + c_{66}\epsilon_{xy}$$

Equations (1) are the mathematical expression of a three-dimensional media with c_{mn} constants being the elastic constants. This means stress $= (c_{mn})$ (strain) and is a statement of Hooke's law. For an isotropic solid Equations (1) reduce to two independent constants since properties are independent of direction, axis rotation, and axis sense.

$$c_{14} = c_{25} = c_{24} = c_{34} = c_{35} = c_{36} = c_{15} = c_{16} = c_{26} = 0$$

$$c_{45} = c_{46} = c_{56} = 0$$

$$2c_{44} = c_{11} - c_{12}$$

(2)

$$c_{11} = c_{22} = c_{33} \qquad c_{44} = c_{55} = c_{66}$$

$$c_{12} = c_{13} = c_{23} \qquad c_{15} = c_{16} = c_{26}$$

$$c_{14} = c_{25} = c_{36} \qquad c_{45} = c_{46} = c_{56}$$

Equations (2) require mathematically that the media be independent of direction, sense and rotation. With the restrictions of Equations (2), Equations (1) reduce to the following equations.

$$\sigma_{xx} = c_{11}\epsilon_{xx} + c_{12}\epsilon_{yy} + c_{12}\epsilon_{zz}$$

$$\sigma_{yy} = c_{12}\epsilon_{xx} + c_{11}\epsilon_{yy} + c_{12}\epsilon_{zz}$$

$$\sigma_{zz} = c_{12}\epsilon_{xx} + c_{12}\epsilon_{yy} + c_{11}\epsilon_{zz}$$

(3)

$$\sigma_{yz} = c_{44}\epsilon_{yz}$$

$$\sigma_{zx} = c_{44}\epsilon_{zx}$$

$$\sigma_{xy} = c_{44}\epsilon_{xy}$$

Now,

$$c_{11} = c_{22} = c_{33} = \lambda + 2\mu ;$$

$$c_{44} = c_{55} = c_{66} = \mu ;$$

$$c_{12} = c_{13} = c_{23} = c_{21} = c_{31} = c_{32} = \lambda .$$

Equations (3) then reduce to the following:

$$\sigma_{xx} = (\lambda + 2\mu)e_{xx} + \lambda e_{yy} + \lambda e_{zz}$$

$$\sigma_{yy} = \lambda e_{xx} + (\lambda + 2\mu)e_{yy} + \lambda_{zz}$$

$$\sigma_{zz} = \lambda e_{xx} + \lambda e_{yy} + (\lambda + 2\mu)e_{zz}$$

$$\sigma_{yz} = \mu e_{yz}$$

$$\sigma_{zx} = \mu e_{zx}$$

$$\sigma_{xy} = \mu e_{xy}$$

(4)

Some other common elastic constants commonly used in conjunction with elastic isotropic solids are Young's modulus, Poisson's ratio, and bulk modulus.

Young's modulus (E) is defined as the ratio of force per unit area of a uniform rod divided by the unit elongation. Both stress and unit elongation (strain) are measured in the direction of the force. The definition requires zero stress in the other two directions as there is no load applied. Also, no loads are applied to cause a shear deformation. From Equations (4) these conditions appear as follows:

$$\sigma_{xx} = (\lambda + 2\mu)e_{xx} + \lambda e_{yy} + \lambda e_{zz}$$

$$0 = \lambda e_{xx} + (\lambda + 2\mu)e_{yy} + \lambda e_{zz}$$

$$0 = \lambda e_{xx} + \lambda e_{yy} + (\lambda + 2\mu)e_{zz}$$

$$0 = \mu e_{yz}$$

$$0 = \mu e_{zx}$$

$$0 = \mu e_{xy}$$

(5)

When one solves Equations (5) with $E = \sigma_{xx}/\epsilon_{xx}$, the following expression results:

$$E = \frac{\mu(3\lambda + 2\mu)}{\lambda + \mu} . \qquad (6)$$

By definition Poisson's ratio (δ) is the ratio of lateral contraction to longitudinal extension or $\delta = \epsilon_{yy}/\epsilon_{xx}$.

From Equations (5)

$$\delta = \frac{\lambda}{2(\lambda + \mu)} . \qquad (7)$$

The bulk modulus K is defined as the ratio of the hydrostatic pressure on a body to the resulting fractional decrease in volume. This situation results when $\sigma_{xx} = -p$, $\sigma_{yy} = -p$, and $\sigma_{zz} = -p$, where p = hydrostatic pressure.

$$-p = (\lambda + 2\mu)\epsilon_{xx} + \lambda\epsilon_{yy} + \lambda\epsilon_{zz}$$

$$-p = \lambda\epsilon_{xx} + (\lambda + 2\mu)\epsilon_{yy} + \lambda\epsilon_{zz} \qquad (8)$$

$$-p = \lambda\epsilon_{xx} + \lambda\epsilon_{yy} + (\lambda + 2\mu)\epsilon_{zz}$$

All shearing stress $= 0$

When one solves Equations (8), $K = -p/\epsilon_{xx} + \epsilon_{yy} + \epsilon_{zz}$;

$$k = \lambda + 2/3\ \mu . \qquad (9)$$

The shear modulus or mudulus of rigidity is simply the Lamé constant.

Several vibrational modes of a wave can propagate in a solid. These modes are termed shear, surface, and compressional waves. Another mode of less importance here is the Lamb wave. A shear wave is commonly called a distortional wave because it causes a shear distortion in an infinitesmal

volume through which it passes. This requires that particle velocity be in a direction perpendicular to the direction of wave travel. This also requires that shear distortion be in a single direction, and this condition requires that the shear wave be polarized in the same manner as polarized light which is used in photoelasticity. The polarized shear wave could penetrate an opaque solid in an analogous manner to the penetration of a transparent solid by plane polarized coherent light.

A longitudinal or compressional wave is a non-distortional wave; i.e., it does not distort the infinitesimal volume of the cube in a shear manner. There are two distinct wave velocities of a compressional wave—bulk velocity and thin rod velocity. The determination of which velocity exists in a solid is made by sample geometry. If the sample is a rod, the wave propagation velocity will be the thin rod velocity if the diameter approaches a wavelength or less in size. If the wavelength is considerably less than the diameter of the rod, the wave velocity will be a bulk velocity. The wave velocity will be independent of actual shape of the solid provided the cross section of the solid is much larger than both the beam cross section and the wavelength of the wave.

The wavelength, velocity of wave propagation, and frequency of oscillation are mathematically related by the following equation

$$v = f\lambda . \tag{10}$$

Where λ is the wavelength in inches, v is the velocity of wave propagation in inches per second, and f is the frequency of oscillation in cycles per second. Other units may be used as long as they are consistent.

In the calculation of acoustic velocities, an absolute consistent set of units makes the calculations easier. The c.g.s. system is recommended.

The moduli would be in dynes per square centimeter, the density would be in grams per cubic centimeter, the velocity in centimeters per second, etc.

V_o is the thin rod velocity, V_ℓ is the longitudinal wave velocity, and V_s is the shear wave velocity. Also, δ is Poisson's ratio, E is the modulus of elasticity, μ is the shear modulus, ρ is the density, and K is the bulk modulus. The following expressions for wave propagation can then be written:

$$V_o = \sqrt{\frac{E}{\rho}}$$

$$V_\ell = \sqrt{\frac{E}{\rho}\frac{(1+\delta)}{(1+\delta)(1-2\delta)}} = \sqrt{\frac{K + 3/4\,\mu}{\rho}}$$

$$V_s = \sqrt{\frac{E}{\rho}\frac{1}{2(1+\delta)}} = \sqrt{\frac{\mu}{\rho}}$$

$$\delta = \frac{1 - 2(V_s/V_\ell)^2}{2 - 2(V_s/V_\ell)^2}$$

$$\mu = \rho V_s^2$$

$$E = \rho V_o^2 = V_\ell^2 \rho \frac{(1+\delta)(1-2\delta)}{1-\delta}$$

$$E = 2\mu(1+\delta) = 3K(1-2\delta) = \frac{9K\mu}{\mu + 3K}$$

$$Z = \rho V = \text{acoustic impedance}\ .$$

(11)

The preceding equations refer to the group velocity of the ultrasonic wave packet. If the material through which the wave propagates is a "lossy" or viscoelastic media, then the moduli and damping terms become

complex when referred to a common reference point. The expressions for these conditions are as follows:

α = attenuation in nepers/centimeter

μ = shear modulus in dynes/cm^2

μ' = shear viscosity in dyne-sec/cm^2

E = Young's modulus in dynes/cm^2

E' = normal viscosity in dyne-sec/cm^2

ω = angular frequency in radians per second

$\bar{\mu}$ = $\mu + j\omega\mu'$ = complex shear modulus

$\bar{E}$ = $E + j\omega E'$ = complex modulus

For Bulk Waves

composite bulk modulus = $K + 4/3\ \mu$

composite viscosity = $K' + 4/3\ \mu'$

K' = bulk viscosity

v = group wave velocity as measured ultrasonically

For Shear Waves

$$\mu = \rho v^2 \frac{1 - \left(\frac{\alpha v}{\omega}\right)^2}{\left[1 + \left(\frac{\alpha v}{\omega}\right)^2\right]^2}$$

$$\omega\mu' = \rho v^2 \frac{2\left(\frac{\alpha v}{\omega}\right)}{\left[1 + \left(\frac{\alpha v}{\omega}\right)^2\right]^2}$$

For Thin Rods or Strips

$$E = \rho v^2 \frac{1 - \left(\frac{\alpha v}{\omega}\right)^2}{\left[1 + \left(\frac{\alpha v}{\omega}\right)^2\right]^2}$$

$$\omega E' = \rho v^2 \; \frac{2\left(\frac{\alpha v}{\omega}\right)}{\left[1 + \left(\frac{\alpha v}{\omega}\right)^2\right]^2}$$

For Bulk Waves

$$K + \frac{4}{3}\mu = \rho v^2 \; \frac{1 - \left(\frac{\alpha v}{\omega}\right)^2}{\left[1 + \left(\frac{\alpha v}{\omega}\right)^2\right]^2}$$

$$\omega\left(K' + \frac{4}{3}\mu'\right) = \rho v^2 \; \frac{2\left(\frac{\alpha v}{\omega}\right)}{\left[1 + \left(\frac{\alpha v}{\omega}\right)^2\right]^2} \; .$$

APPENDIX B

DYNAMIC PROPERTY ERROR FOR A GIVEN ERROR

IN ATTENUATION MEASUREMENT

In Chapter III a series of possibilities were stated which concerned the reflection, refraction, mode conversion, and beam spreading (divergence) of an ultrasonic wave. Each of these possibilities could divert a portion of the energy of the wave packet and falsely indicate more attenuation of the wave amplitude than exists.

In actual ultrasonic testing the mode conversion at the buffer block-sample interface creates a longitudinal wave of substantial amplitude. Since all of the factors mentioned in the first paragraph tend to introduce error in the attenuation measurements of the wave and not in the velocity calculations, a typical case was selected, and the error determined for a given error in attenuation measurement. From Equations (12) the following equations result.

$$\overline{E} = E + j\omega E'$$

where

$$E = \frac{\rho v^2 \left[1 - \left(\frac{\alpha v}{\omega} \right)^2 \right]}{\left[1 + \left(\frac{\alpha v}{\omega} \right)^2 \right]^2}, \qquad \omega E' = \frac{2\rho v^2 \left(\frac{\alpha v}{\omega} \right)}{\left[1 + \left(\frac{\alpha v}{\omega} \right)^2 \right]^2}$$

v is the measured group velocity determined with X-cut quartz crystals. Also,

$$\frac{\omega E'}{E} = \frac{2\left(\dfrac{\alpha v}{\omega}\right)}{1 - \left(\dfrac{\alpha v}{\omega}\right)^2} = \tan\theta .$$

When one takes the derivative with respect to α, the following equation results:

$$\frac{d\left(\dfrac{\omega E'}{E}\right)}{\dfrac{\omega E'}{E}} = \frac{1 + \dfrac{\alpha^2 v^2}{\omega^2}}{1 - \dfrac{\alpha^2 v^2}{\omega^2}}\frac{d\alpha}{\alpha} = \frac{d\,(\tan\theta)}{\theta} .$$

If one assumes a measurement error of 20% in the determination of α, this defines $\dfrac{d\alpha}{\alpha} = 0.2$. Also, If one selects a lossy material whose wave velocity is $v = 190,000$ cm/sec, the above equation then reduces to the following:

$$\frac{d\left(\dfrac{\omega E'}{E}\right)}{\dfrac{\omega E'}{E}} = \frac{1 + \left(\dfrac{\alpha}{f}\right)^2 9.18 \times 10^8}{1 - \left(\dfrac{\alpha}{f}\right)^2 9.18 \times 10^8} (0.2) .$$

If one assumes a frequency of 500,000 cycles per second and an attenuation of 100 nepers/cm, the equation reduces to the following:

$$\frac{d\,(\tan\theta)}{\theta} = \frac{d\left(\dfrac{\omega E'}{E}\right)}{\dfrac{\omega E'}{E}} = \frac{1 + 36.6}{1 - 36.6} (0.2) \doteq -0.2 .$$

Or, this indicates that the error in the calculation of the phase angle between stress and strain is of the same magnitude as the attenuation error but in the opposite sense. The angle θ is normally determined in a test of a lossy material in a dynamic test using a vibration exciter. For the above assumed material, the error in θ approaches $-.20$ more closely for low frequencies that for a frequency of 500,000 cps. The same case holds approximately true for frequencies of many megacycles.

The equations or relations for error in the complex shear modulus are the same as for the complex modulus.

In many cases the complex moduli are not calculated, and only Young's modulus and the modulus of rigidity are determined. The error relationships for these cases are derived as follows: from Equations (11),

$$V_s = \sqrt{\mu/\rho} \quad \text{and} \quad V_\ell = \sqrt{E/\rho}.$$

A more specific form of these equations is:

$$\sqrt{\frac{E}{\rho}} = |c_1 - ic_2| = c^* \quad \text{(the velocity modulus)}.$$

$$\sqrt{\frac{E}{\rho}} = \left| \frac{v}{1 + \left(\frac{\alpha v}{\omega}\right)^2} - \frac{iv\left(\frac{\alpha v}{\omega}\right)}{1 + \left(\frac{\alpha v}{\omega}\right)^2} \right|$$

$$= \sqrt{\left(\frac{v}{1 + \left(\frac{\alpha v}{\omega}\right)^2}\right)^2 + \left(\frac{v\left(\frac{\alpha v}{\omega}\right)}{1 + \left(\frac{\alpha v}{\omega}\right)^2}\right)^2}$$

$$\frac{E}{\rho} = \frac{v^2}{1 + \left(\frac{\alpha v}{\omega}\right)^2}$$

$$\frac{dE}{E} = \frac{-2\left(\frac{\alpha v}{\omega}\right) d\left(\frac{\alpha v}{\omega}\right)}{1 + \left(\frac{\alpha v}{\omega}\right)^2}$$

$$\frac{dE}{E} = \frac{-2}{1 + \frac{1}{\left(\frac{\alpha v}{2\pi f}\right)^2}} \frac{d\alpha}{\alpha}.$$

If one takes the case of a material whose v is 190,000 cm/sec and whose attenuation is 100 nepers/cm, and assumes the test frequency is 500,000 cps., the following error relationships results:

$$\frac{dE}{E} = \frac{-2}{1 + \frac{1}{36.6}} \frac{d\alpha}{\alpha}$$

$$\frac{dE}{E} \doteq -2 \frac{d\alpha}{\alpha} .$$

This indicates that for a given error percentage in α, the percentage of error in E will be twice as great and in the opposite sense.

The same condition is prevalent for the shear modulus.

It can be seen, therefore, that an error in the determination of the attenuation of a wave can introduce an error of the same magnitude or greater in calculation of moduli. This result has prompted the development of special test techniques in ultrasonics which tend to reduce such measurement errors. The interferometer technique with different sample thicknesses in each path is one of the better test methods for decreasing attenuation error.

Sample Calculations

1. For velocity of 100-0 composition urethane

$$V_\ell = \frac{0.156 \text{ inches}}{1.75 \times 10^{-6} \text{ seconds}} = 89,100 \text{ in/sec}$$

$$V_s = \frac{0.156 \text{ inches}}{4.51 \times 10^{-6} \text{ seconds}} = 34,600 \text{ in/sec}$$

2. For attenuation of 100-0 composition urethane

$$\left.\frac{db}{in}\right)_{shear} = \frac{20 \log V_2/V_1}{length} = \frac{20 \log 0.0667}{0.156 \text{ inches}} = -150$$

Since attenuation infers a decrease, the negative sign is ignored.

$$\frac{db}{in}\Bigg)_{shear} = 150$$

$$\frac{Nepers}{cm}\Bigg)_{shear} = \frac{\ln V_2/V_1}{length} = \frac{\ln 0.0667}{0.156 \times 2.54} = 6.84$$

3. Calculation of E for 100-0 composition urethane:

$$E = \rho v^2 \frac{1 - \left(\frac{\alpha v}{w}\right)^2}{\left[1 + \left(\frac{\alpha v}{w}\right)^2\right]^2}$$

$$E = \rho v^2 \frac{1 - \left(\frac{3.41 \times 226{,}000}{2\pi \times 2.25 \times 10^6}\right)^2}{\left[1 + \left(\frac{3.41 \times 226{,}000}{2\pi \times 2.25 \times 10^6}\right)^2\right]^2}$$

$$E = (.099) \, \rho v^2$$

$$E = \left[1.134 \, \frac{gm}{cm^3} \cdot \frac{1 \, lb}{454 \, gm} \cdot \frac{(2.54)^3 \, cm^3}{1 \, in^3} \cdot \frac{1 \, sec^2}{386 \, in}\right] (.99) \, v^2$$

$$E = \left[1.06 \times 10^{-4} \, \frac{lb\text{-}sec^2}{in^4}\right] (.99)(89{,}100)^2 \, \frac{in^2}{sec^2}$$

$$E = 83.3 \times 10^4 \, \frac{lb}{in^2}$$

$$E = 833{,}000 \, \frac{lb}{in^2}$$

4. Calculation of $\omega E'$ for 100-0 composition urethane:

$$\omega E' = \rho v^2 \frac{2\left(\frac{\alpha v}{\omega}\right)}{\left[1 + \left(\frac{\alpha v}{\omega}\right)^2\right]^2}$$

$$\omega E' = \rho v^2 \quad \frac{2(.0425)}{\left[1 + \left(\frac{6.84 \times 87,900}{6.28 \times 2.25 \times 10^6}\right)^2\right]^2}$$

$$\omega E' = 2\rho v^2 (.0422)$$

$$\omega E' = \frac{2(1.134)(2.54)^3(34,600)^2(.0422)}{(454)(386)}$$

$$\omega E' = 10,730 \text{ psi}$$

$$\overline{E} = E + j\omega E'$$

$$\overline{E} = 833,000 + j\ 10,730 \text{ psi}$$

for 100-0 formulation

APPENDIX C

SELECTED TEST RESULTS

The following oscilloscope traces are shown to illustrate the wave-
forms received. The different waves received are shown versus time. A
high degree of interpretation is often necessary to identify a given
wave. The time setting on the oscilloscope was 10 u sec/cm unless other-
wise noted. Temperature was $80°F \pm 2°$. Y-cut 2.25 megacycle quartz
crystals generate the acoustic wave.

Velocity Measurements
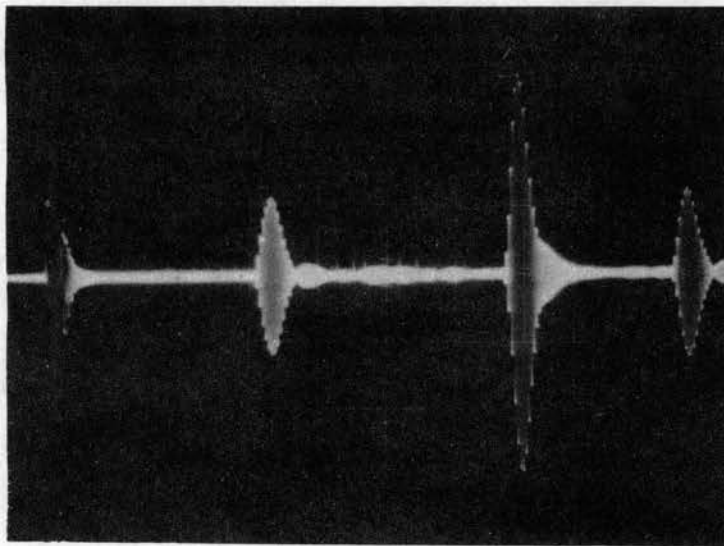
Figure 15. Buffer Block Reference.

77

78
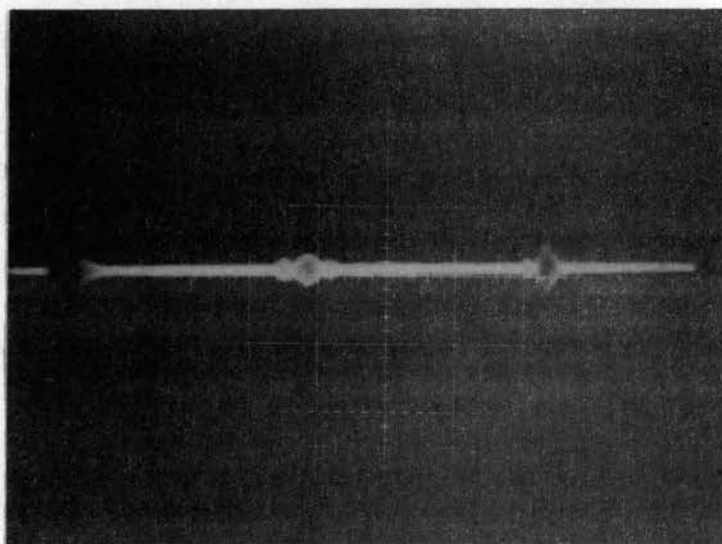
Figure 16. 40-60 Formulation Urethane.
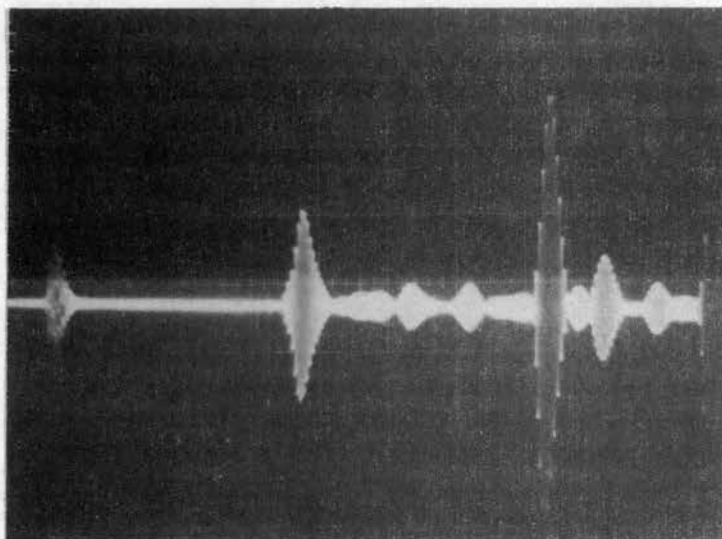
Figure 17. 1.00 inch Aluminum Block.

In the buffer block reference trace picture, the far left signal is
the radiated initial pulse. The second signal is the longitudinal wave
generated by the Y-cut crystal. The third signal is the generated shear
wave, and the fourth signal is the first reflection within the buffer
block of the generated longitudinal wave. The longitudinal and shear
waves are generated simultaneously by the sending crystal.

Wave Attenuation Comments

Both longitudinal and shear waves existed so both measurements
could be made. The pictures were typical in representing the appearance
of the oscilloscope traces. In general the oscilloscope time base was
10 u sec/cm.
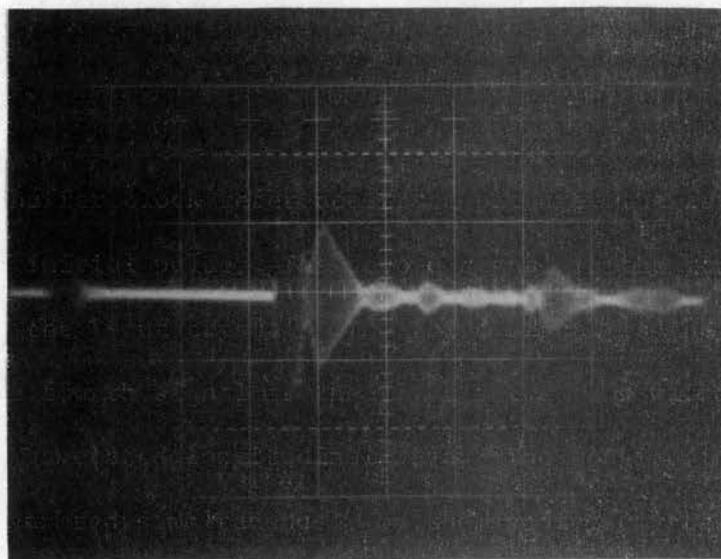
Figure 18. 100-0 Formulation Urethane.
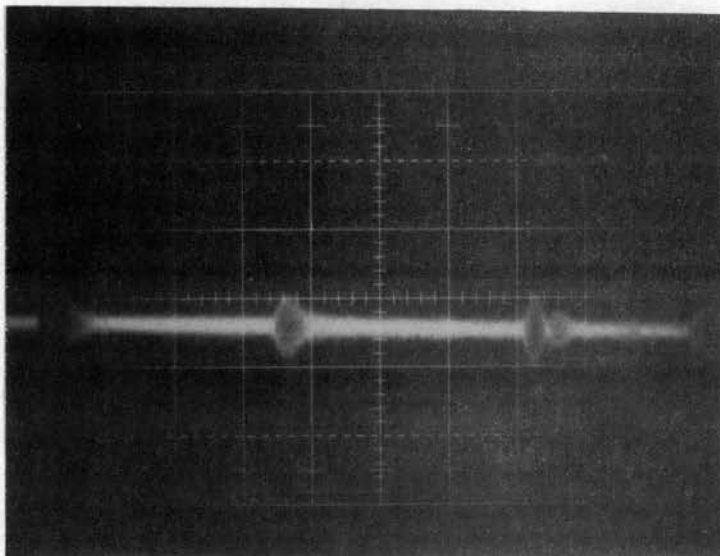
Figure 19. 55-45 Formulation Urethane.

Wave Attenuation
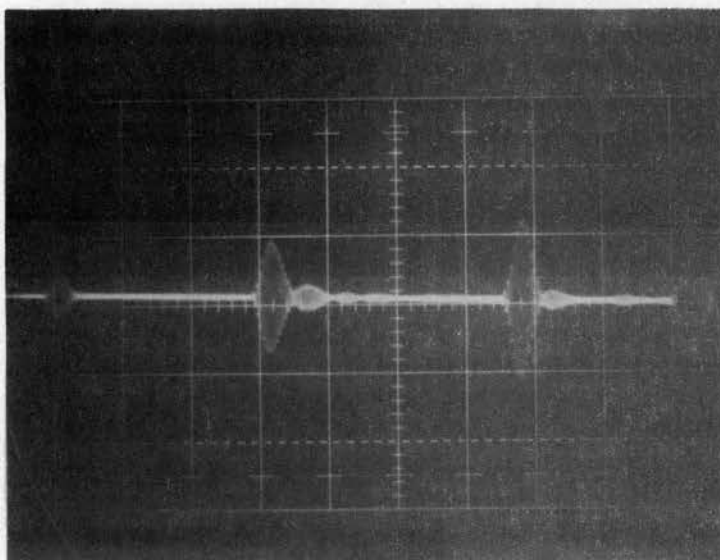
Figure 20. 100-0 Formulation Urethane Refer-
ence 0.01 v/cm.
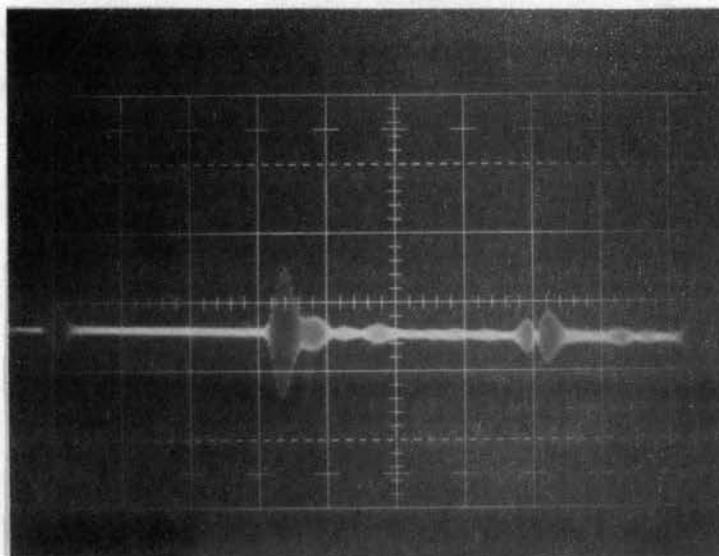
Figure 21. 100-0 Formulation Urethane 0.002
v/cm.
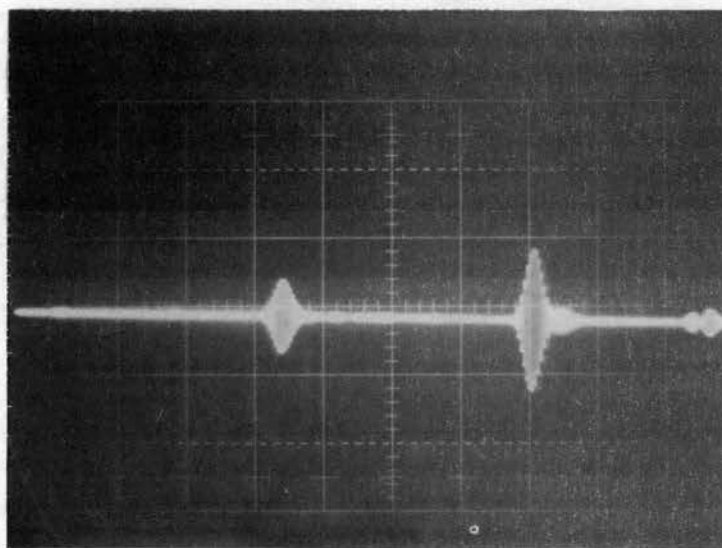
Figure 22. 55-45 Formulation Urethane Refer-
ence 0.1 v/cm.
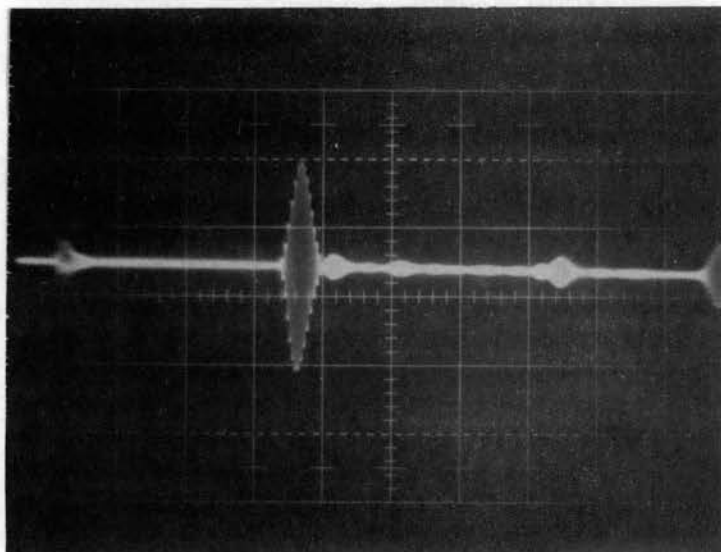
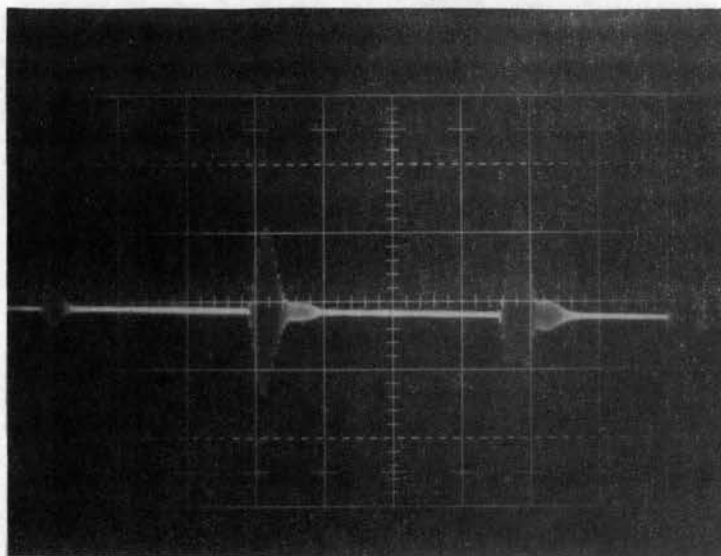Figure 23. 55-45 Formulation Urethane 0.005
v/cm.

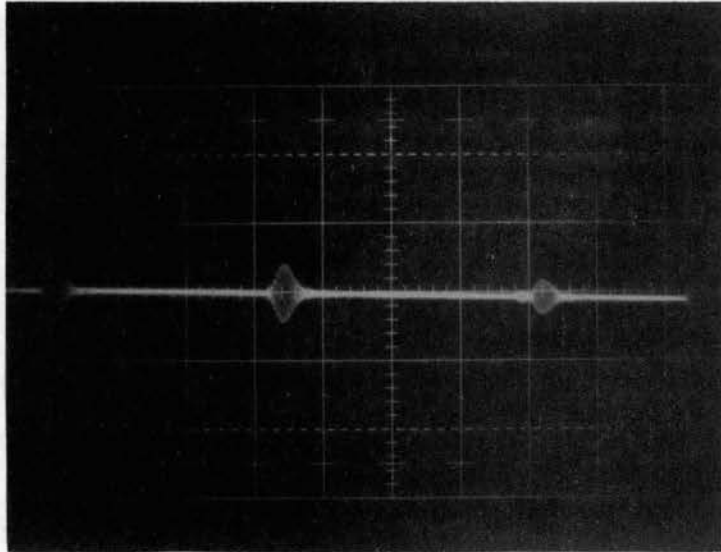Figure 24. 25-75 Formulation Urethane Refer-
ence 0.02 v/cm.

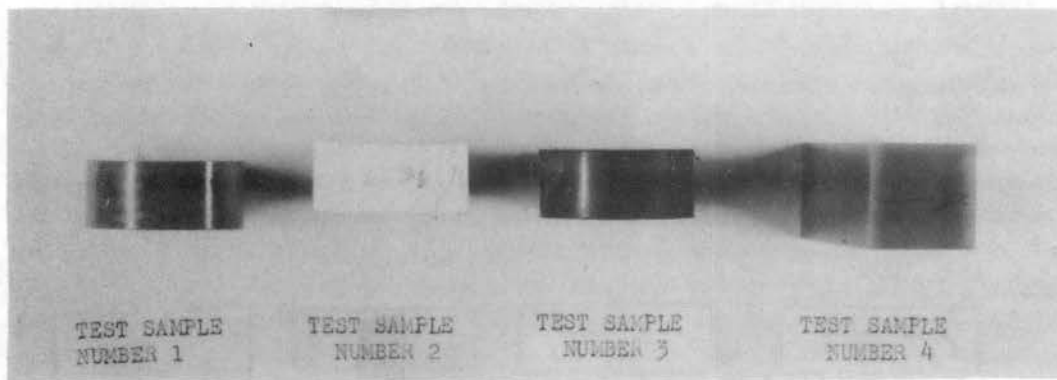Figure 25. 25-75 **Formu**lation Urethane 0.005 v/cm.

TEST SAMPLE NUMBER 1   TEST SAMPLE NUMBER 2   TEST SAMPLE NUMBER 3   TEST SAMPLE NUMBER 4

Figure 26. Rubber and Hard Plastic Test Samples.

The picture above shows the three silicon rubber samples and the unknown plastic sample tested. The oscilloscope trace of the received signal is shown for each sample in the following pictures.
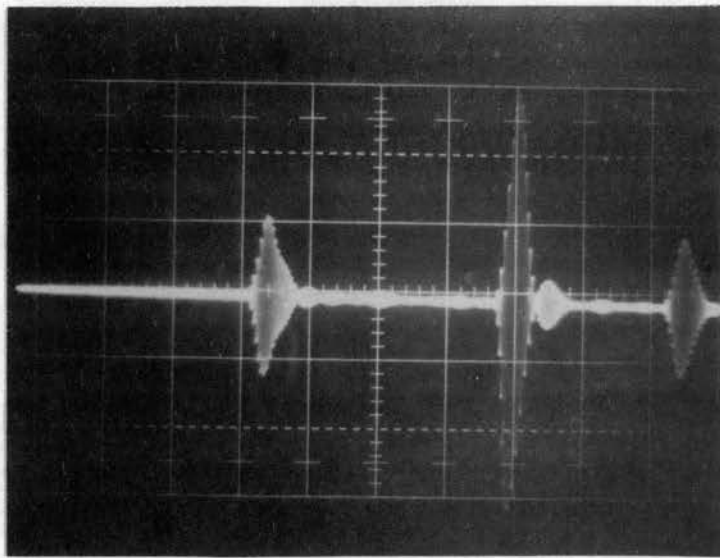
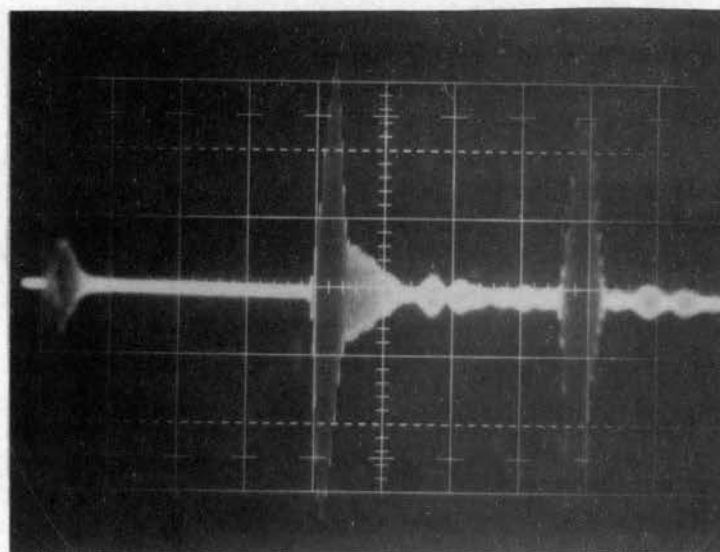Figure 27. Reference for Test Sample Number 1
(Rubber) 0.05 v/cm.

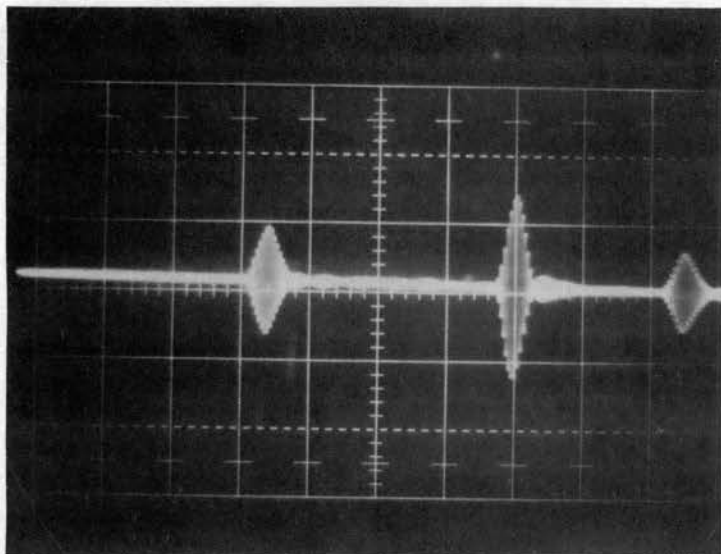Figure 28. Test Sample Number 1. 0.001 v/cm.

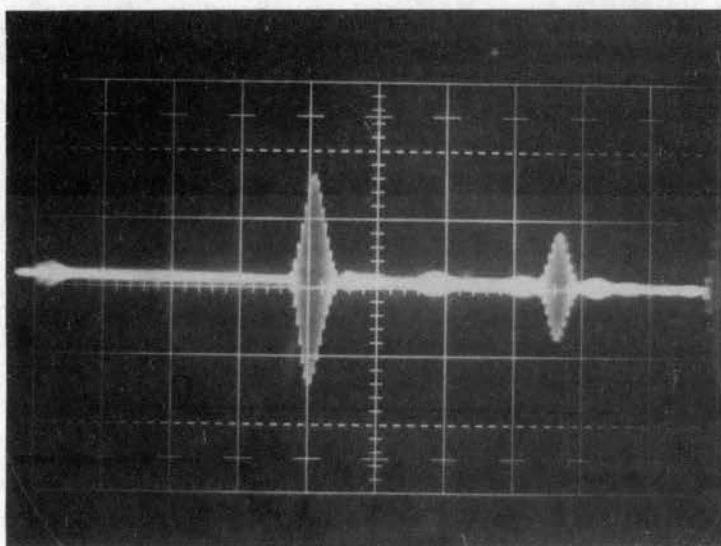Figure 29. Test Sample Number 4 (Hard Plastic)
0.1 v/cm.

Figure 30. Test Sample Number 4. 0.005 v/cm.

APPENDIX D

GLOSSARY OF SELECTED TERMS

1. <u>Characteristic Impedance.</u> The characteristic impedance of a trans-
mission line is that impedance that could be placed across the
cut end of an infinitely long line and cause no reflection at
the source.

2. <u>Couplant.</u> A couplant here is understood to mean a medium located
between two media which enables ultrasonic wave propagation from
one medium to the other.

3. <u>Gated Sine Wave.</u> A gated sine wave is a sine wave which has a defi-
nite number of cycles or a definite fraction of cycles. It has
no starting or stopping transients.

4. <u>Lossy Material.</u> A lossy material is a material that severely damps
the amplitude of an acoustic wave which propagates through it.

5. <u>Q-Factor.</u> The Q of a circuit is the ratio of maximum energy of
oscillation stored in a cycle to the maximum energy dissipated
in a cycle.

VITA

O'Neill James Burchett

Candidate for the Degree of

Doctor of Philosophy

Thesis: TIME DOMAIN REFLECTOMETRY FOR MEASURING VISCOELASTIC PROPERTIES

Major Field: Mechanical Engineering

Biographical:

 Personal Data: Born near Seiling, Oklahoma, June 11, 1935, the son
    of Roy and Louise Burchett.

 Education: Graduated from Seiling High School, Seiling, Oklahoma,
    1953; received the Bachelor of Science Degree in Mechanical
    Engineering from Oklahoma State University in May, 1958; received
    the Master of Science Degree in Mechanical Engineering from
    Oklahoma State University in May, 1960; completed requirements
    for Doctor of Philosophy Degree in May, 1966.

 Professional Experience: Employed six years as a teacher and research
    engineer at Oklahoma State University